# PROCESSING AND CHARACTERIZATION OF POROUS ALUMINA CERAMICS WITH WIDE POROSITY RANGE

*A thesis submitted in partial fulfillment of the*
*Requirement for the degree of*

## MASTER OF TECHNOLOGY (RESEARCH)

By

**CHELLURI SOWJANYA**
**(Roll no. 612CR301)**

*Under the guidance of*

**Prof. Swadesh Kumar Pratihar**

and

**Prof. Santanu Bhattacharyya**


**DEPARTMENT OF CERAMIC ENGINEERING**

**NATIONAL INSTITUTE OF TECHNOLOGY, ROURKELA**

**DECEMBER 2014**

Department of Ceramic Engineering
NATIONAL INSTITUTE OF TECHNOLOGY,
ROURKELA
Orissa-769008

# CERTIFICATE

This is to certify that the thesis entitled **"Processing and Characterization of Porous Alumina Ceramics with Wide Porosity Range,"** submitted by **Miss Chelluri Sowjanya** for the degree of **Master of Technology (Research)** in **Ceramic Engineering** to the National Institute of Technology, Rourkela is a record of bonafide research work carried out by her under our supervision and guidance. Her thesis, in our opinion, is worthy of consideration for the award of degree of Master of Technology (Research) in accordance with the regulations of the institute.

The results embodied in this thesis have not been submitted to any other university or institute for the award of a Degree.

**Prof. Santanu Bhattachayya**
Professor
Department of Ceramic Engineering
National Institute of Technology
Rourkela

**Prof. Swadesh Kumar Pratihar**
Associate professor
Department of Ceramic Engineering
National Institute of Technology
Rourkela

# Table of contents

## Acknowledgements

This dissertation would not have been possible without the guidance and the help of several individuals who in one way or another contributed and extended their valuable assistance in the preparation and completion of this study.

Foremost, I would like to express my sincere gratitude to my advisors Prof. Swadesh Kumar Pratihar and Prof. Santanu Bhattacharyya for the continuous support of my M.Tech(R) study and research, for their patience, motivation, enthusiasm, and immense knowledge. I attribute the level of my Master's degree to their encouragement and effort and without them this thesis, too, would not have been completed or written. One simply could not wish for better or friendlier supervisors.

I express my sincere thanks to Prof. Swadesh Pratihar, Head of Ceramic Engineering for providing me all the departmental facilities required for the completion of the thesis. His out of the way help and guidance helped the thesis to reach the final shape. I am also thankful to all other faculty members of Ceramic Engineering Department, NIT Rourkela for their invaluable advice, constant help, encouragement, inspiration and blessings.

I am also indebted to my senior research colleagues Nadiya bhai, Sarat bhai, Subrat Bhai, Ganesh Bhai, Sanjay bhai, Gita deedi, Smruti deedi, Jayarao bhai, Abhisek bhai, Sangeeta deedi and Raju bhai for their unconditional support and constant motivation whenever needed. I am very grateful to all my dear friends Abhinay, Soumya, Prativa, Sreenivas and Venkatesh who have given me their friendship, put up with my odd hours, and provided me with lifts and practical help. Last but not the least, I would like to thank my dear parents and brother for their support.

Chelluri Sowjanya

## Abstract

In recent years, porous ceramics with tailored microstructure has received wide attention in the research communities for its specialized properties. To have a customized microstructure suitable for different applications, several fabrication methods have also been developed during the last decades to manipulate porosity, pore size distribution and pore interconnectivity in the porous ceramics. In the present study, an attempt has been made to develop porous alumina ceramics with wide porosity (10-80%) using three different fabrication methods. The three methods are starch consolidation casting (SCC), polymeric sponge replica technique (SRT) as well as the combination of the two methods (SCC+SRT). A theoretical model has also been developed and validated with the experimental data to predict the porosity of the samples prepared by SCC theoretically. Alumina loading, starch content, starch types are used as the tools to develop different porosity in the samples made by starch consolidation casting. $TiO_2$ has been used as sintering additives to improve high strength in the starch consolidated samples without compromising the porosity. The viscosity of the slurry in the range 0.05-1.19 Pa.s was found to be optimum to fabricate defect free samples by starch consolidation casting. The porosity of the samples could be varied from 20-70% in this technique. $TiO_2$ as sintering aid was able to reduce the sintering temperature of the samples in the tune of 300$^oC$ without compromising the strength and porosity of the samples fabricated by this technique. It was observed that 10% porous samples could be developed through this technique. Particle loading of the slurry was found as an important parameter to develop different pore morphology when the samples prepared using sponge replica technique. The porosity of the samples could be varied from 75- 80% of strength 0.31-2.46 MPa by this technique. An attempt has also been made to develop hierarchical porosity in the samples while fabricated by the combination of the above two techniques. The microstructural study revealed the formation of hierarchical porosity in the samples fabricated by the combination technique. Thus, porous ceramics with porosity in the range these techniques could achieve 10-80%.

# List of figures

# List of tables

# Chapter 1 Introduction

The research interest in the field of porous ceramics has increased in the recent decade. Improved and innovative processing of porous ceramics has led to the development of customized microstructural features. Porosity, pore size distribution in a low-density body can be well controlled to obtain a proper combination of strength, low thermal conductivity, high specific surface area and high permeability [1]. These porous ceramics are suitable for wide range of technical applications. The applications include catalyst supports, filters for molten metals and diesel engine exhaust, burners, biomedical device, kiln furniture and high-temperature thermal insulation, etc. [2-4]. Several fabrication techniques have been developed in order to meet the requirements of the desired properties for different applications. The techniques are sacrificial template method [5, 6], paste extrusion [7], freeze casting [8], direct foaming [9, 10], replica technique, rapid prototyping etc. [11-12]. Different fabrication techniques have their advantages and limitations.

Starch consolidation casting (SCC) belongs to the family of sacrificial template method. The sacrificial template technique consists of a biphasic composite with a continuous matrix of ceramic particles and a dispersed sacrificial phase that is homogeneously dispersed throughout the matrix and is extracted while sintering to generate pores in the microstructure. Starch is used as pore former and body consolidator utilizing its swelling/gelling properties. The gelling properties of the starch were enhanced by the presence of the linear polymer chain amylose and branched polymer chain amylopectin present in the starch structure [14]. The porosity and pore size distribution of the porous body depends on the starch type, starch amount, the viscosity of the slurry, particle size distribution of the ceramic powder, etc. Sample with porosity 60-70% could be achieved in this technique. In the polymeric Sponge Replica Technique (SRT), the polymeric sponge is impregnated with a ceramic slurry. Subsequently, the excess slurry is removed to produce a positive morphology of the original template [15]. SRT is suitable to produce porosity 80-90% in the sintered sample. The porosity is mainly controlled by the rheology of the ceramic slurry and the porosity/pore morphology of the sponge. Porous alumina ceramics with 10-80% porosity has been fabricated and characterized following SCC and SRT. The present study deals with the fabrication and characterization of porous alumina ceramics following SCC, SRT and combination of these two techniques.

The structure of the thesis is as follows. The literature review in Chapter 2 consists of four parts. The first section summarizes the importance of porous ceramics, its present fabrication techniques, and applications. The second section shows the stabilization of the slurry required for processing through starch consolidation and the polymeric replica technique. The third part introduces the starch consolidation and the importance of each step from the processing to the sintering on the properties of the final product. The fourth section gives the detailed idea on the polymeric sponge replica technique and its properties.

Chapter 3 explains the objective of the present work. Chapter 4 describes the experimental methods involved in the present study, which includes the optimization of the alumina slurry, swelling behavior experimental procedures, characterization procedures related to different properties of the final product. Chapter 5 discusses the predicted model for the generation of porosity in the starch consolidation casting assuming certain parameters are not affecting the system.

The results and discussion of Chapter 6 have been divided into five parts. The first part summarizes the raw material characterization, i.e., the particle size, microstructure and thermal properties of the starting materials. The second part discusses the optimization of the alumina slurry using Darvan C as a dispersant. The third part explains the effect of alumina loading and the starch content on the properties of porous alumina ceramics through starch consolidation casting. The Fourth part gives the idea of the impact of solid loading on the rheological and mechanical properties of the porous samples prepared by polymeric sponge replica technique. Fifth part introduces the new processing technique by combining the starch consolidation casting and the polymeric sponge replica technique that produces a hierarchical pore structure. Chapter 7 summarizes the main findings and the conclusions of the present study.

# Chapter 2 Literature Review

## 2.1. Introduction to Porous Ceramics

The production and application of highly porous ceramics have increased in the recent decades due to their tailored microstructure like porosity and pore size distribution. These porous ceramics are more suitable for wide range of technical applications. They are catalyst supports; filters for molten metals and hot gasses; ion exchangers, burners etc. It also includes kiln furniture and high temperature thermal insulation where the high temperature, corrosion resistant and wear resistant environments are involved.

The compositional and microstructural features of cell size, morphology and degree of interconnectedness are primary factors that influence potential applications. The closed cell materials are needed for thermal insulation while the open cell and the interconnected materials are required for filters and catalysts. Pores present in the porous structure are classified into three groups depending on their sizes namely microporous (< 2 nm), mesoporous (2-50 nm) and macroporous (> 50 nm) [16]. Micro and mesoporous ceramic materials are used as molecular sieves [17], in catalysis [18] and controlled release applications [19, 20]. Macroporous ceramics applications starts from traditional ceramics like roof tiles to advanced technical ceramics in medicine and automobile engines [21].

The development of the porous filters satisfied the requirements like the recovery of the methane from mines, removal of carbon dioxide and hydrogen sulfide from natural gas, recovery of hydrogen in petroleum refinery operation. In the foundry industry, porous filters are used for hot metal filtration [22]. Some of the application areas of catalyst supported porous materials are in the mass transfer of the catalytic combustion [23], in-situ combustion in underground reservoirs for enhanced oil recovery, heat transfer devices, diesel particulate filters [24] and reduction of hazardous combustion products. Besides, porous ceramics is also used in sensors, battery materials and thermal protection materials and biomedical applications [25]. The classification of the porous ceramic based on pore structure and its applications is given in the Table II.I.

**Table II.I: Classification of Porous Ceramics Based on Pore Structure and Applications [26].**

| Pore structure | Application |
|---|---|
| Micro and Meso-porous materials | Desiccant materials<br>Sensors and actuators<br>Catalyst support<br>Drug delivery systems, coatings, carriers |
| Foam and honeycomb structures | Exhaust gas filters<br>Diesel particle filters<br>Filters for molten metal<br>Porous electrodes of fuel cells<br>Porous burners<br>Catalytic substrates<br>Biomedical porous scaffolds for tissue engineering<br>Impact and acoustic materials<br>Kiln furniture<br>Lightweight sandwich structures |
| Multilayer materials | Ultra filtration membranes<br>Nano filtration membranes<br>Gas separation membranes<br>Zeolite membranes<br>Pervaporation membranes<br>Dense membranes (oxygen or proton conductors) |

## 2.2. Fabrication of Porous Ceramics

Several fabrication techniques are developed to meet the requirements of the desired properties for particular applications like replica technique, sacrificial template method, direct foaming, paste extrusion, rapid prototyping. Using the replication technique maximum porosity obtained can be in the range of 40-95% and pore size in the range of 200µm to 3mm. High interconnectivity in the structure makes them more advantageous for the filter purposes. The basic disadvantage of this technique is that they have low mechanical strength. Several attempts are made to overcome this by repeated coating and combining the technique with gel casting. Several techniques like starch consolidation casting, gel casting, freeze casting comes under sacrificial template techniques. The name of the technique differs from the application of the type of the fugitives and the difference in the processing steps. The porosity obtained by this technique is in the range of 20-90% having a pore size in the range of 1-100µm. Direct foaming technique results in the porosity of 40-90% with a pore size in the range of 35mm to 1.2 mm and

compressive strength 16MPa. Honeycomb structures with unidirectional channels can be obtained using the paste extrusion method. More complex shapes can be obtained by using the rapid prototyping technique along with the controlling the pore structure. The main disadvantage of the technique is high manufacturing cost. Different fabrication techniques for macroporous ceramics showing porosity amount and pore size has been summarized in Table II.II.

**Table II.II: Fabrication Techniques of Macroporous Ceramics.**

| Fabrication technique | Porosity range (%) | Pore size range |
|---|---|---|
| Polymeric sponge replica [1,15] | 40-90 | 200µm - 3mm |
| Wood replica [1,22] | 25-95 | 10 - 300µm |
| Gel casting [9,10] | 75-86 | 15-150µm |
| Freeze casting [8] | 30-99 | 20-200µm |
| Starch consolidation casting [5,13] | 20-70 | 5-170µm |
| Extrusion [22] | 40-50 | 100-500µm |
| Protein consolidation | 50-70 | 250-500µm |
| Combination of sponge replica and gel casting | 60-85 | 200-400µm |
| Combination of gel casting and sacrificial template method | 84-90 | 100µm-1mm |

## 2.3. Stabilization of the Slurry

The colloidal particles form agglomerates spontaneously in the dispersion medium due to the presence of strong interparticle van-der-Waals attractive forces. It is required to reduce these attractive forces to avoid the aggregation. The reduction in the attractive forces can be achieved by introducing the repulsive forces between the particles. Two mechanisms can achieve this repulsive barrier namely electrostatic stabilization and steric stabilization. In electrostatic stabilization, the repulsion of the particles takes place by the extended layer of electrostatic

charges on the particles called the electrical double layer. When two such particles interact, it is the interaction between the double layers absorbed around the particles producing a repulsive force. The double layer interaction decreases as the concentration of the oppositely charged ions in the medium increases. The steric stabilization can be achieved by the absorption of uncharged polymer chains onto the particle surface. The polyelectrolyte can produce both the stabilization effects called the electro-steric stabilization. Thus in the present study Darvan C is used as dispersant that is a polyelectrolyte [16].

The aqueous alumina suspension stability in the presence of dispersant Darvan C (ammonium salt of polymethacrylic acid) has been studied [11]. Sediment height and turbidity of the slurry was used as a tool to find out optimum dispersant concentration.

Electrostatic stabilization is based on the repulsive force, originated from the surface charge of the particles. Alumina dispersed in aqueous medium shows positive surface charge. Darvan C in aqueous medium dissociates and produces carboxylic (COO-) groups, which absorbed on the alumina particles surface. Thus, negative charges developed on the alumina particles. The magnitude of the negative surface charge on the powder particle increases with the increase in the Darvan C concentration. Thus, the distance between the particles in the suspension increases with the addition of the Darvan C leading to a well dispersed suspension. The study on sedimentation height revealed that 1ml/g Darvan C concentration as the optimum value for the well-dispersed slurry.

Paul F.Luckham studied the rheological behavior of the alumina suspensions in the presence of dispersant (Darvan C) [27]. It has been observed that the viscosity decreases initially and then increases with the increase in the Darvan C concentration. The decrease in the viscosity of the suspension in the presence of Darvan C is attributed to the insufficient surface coverage of the alumina particles by the dispersant molecules. The addition of the excess amount of Darvan C increases the viscosity of the slurry due to the overcrowding effect of the electrolyte and reduces the double layer repulsive forces between the particles. Different forces causing the instability of the slurry was shown in Fig 2.1.

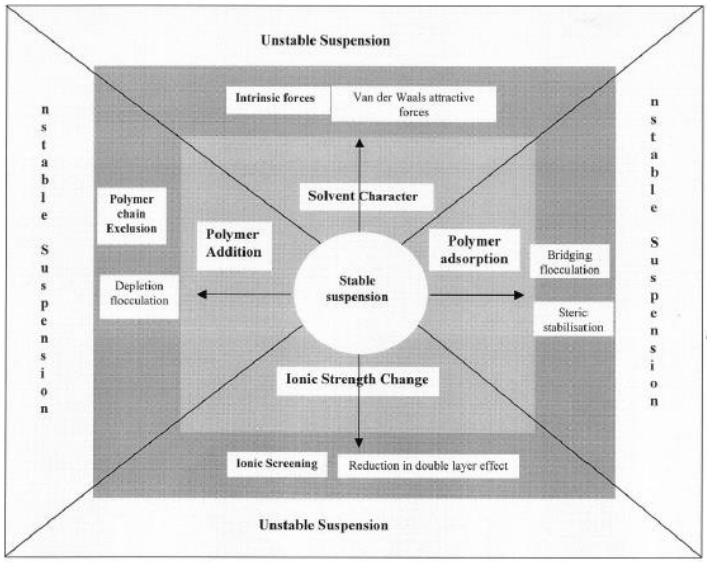


**Figure 2.1: Different forces that cause instability in a stabilized suspension. The arrow direction indicates the increasing of the effect [27].**

The viscosity of colloidal alumina suspensions as a function of dispersant (ammonium polyacrylate, i.e.,.Disperlan LA) concentration was studied [28] for a very narrow range. It has been reported that the viscosity of the slurry followed an exponential decay behaviour. The study revealed that optimum dispersant would be 0.6 vol% for stable colloidal suspension.

The effect of dispersant (polyacrylic ammonium) concentration on the apparent viscosity of the alumina suspension has been studied [29]. It has been observed that the viscosity decreases and then increases gradually with the addition of the dispersant. The minimum viscosity is obtained at 0.36gm per 100gms of alumina that is attributed to the saturated amount of dispersant absorbed onto the powder particles. The sedimentation test were done at 0.16, 0.24, 0.36 and 0.60 dispersant amounts that showed coagulated, well dispersed but under saturation, well dispersed and saturated, weakly coagulated slurry respectively. Hence, the study suggested that the 0.36gm per 100gms of alumina powder is the optimum amount for the well dispersed stable alumina slurry.

The dispersion of the alumina particles using polyvalent electrolyte dispersant (Darvan C) has been optimized [30]. Darvan C is an ammonium salt of polymethacrylate available in the form of the aqueous solution that contains 25% of the active component. The apparent viscosity decreases initially and then increases in which the minimum viscosity is obtained at 1% Darvan

C (related to the alumina powder). The optimum amount of dispersant corresponds to the adsorbed amount and the negligible amount of free dispersant in the continuous phase of the alumina suspension. Any amount of free dispersant acts as a free electrolyte in the system disturbs the electrostatic forces and reduces the double layer repulsive forces giving rise to the increase in the viscosity.

The powder agglomeration in the ceramic slurry can be eliminated with the addition of appropriate dispersant which alters the powder surface properties. The repulsive forces due to electrostatic repulsion results as the overlapping of electrical double layers become higher and thus the particles remain separated in the suspension. Thus, stable slurry could be achieved with the addition of an optimum dispersant amount that imparts low viscosity as well as ensures the dispersion of the powder particles for a long period. Christos Agrafiotis et al., [31] optimized the rheological properties of the alumina slurry at different solid loading as a function of dispersant concentration. It has been observed that the low and intermediate solid loadings exhibit constant and low viscosities, thus indicating that they are independent of the dispersant concentration whereas the high solid loadings are dependent on the dispersant concentration. It has been reported that high viscosity was obtained below 0.075wt% dispersant concentration, the constant viscosity of 97mPas in the region 0.075-0.125wt% and rise in the viscosity was observed above 0.2wt% dispersant concentration.

### 2.4. Starch Consolidation Casting (SCC)

At present among the fabrication techniques, starch consolidation has obtained a great interest in the processing of porous ceramics. The starch granules are dense and water insoluble at room temperature that helps in easy handling without affecting their granular structure. Minor swelling of starch granules occurs due to slight absorption of the moisture in the high humidity conditions but retains their size on drying. In common the starch irrespective of the type has 10-17% moisture in their structure. The size of the starch varies with the type of the starch and generally, their size varies in the range of 2µm to 170µm. The combined advantage of the pore is forming and body forming property of the different type of starch are utilized in this technique [5]. The application of these biopolymer pore formers is widely spread considering certain factors like their non-toxic, eco-friendly, processing nature and controllable porosity [32-33]. These pore formers burn out in the range of 300$^{o}$C to 600$^{o}$C [34].The presence of the linear amylose and

highly branched amylopectin in starch are responsible for the body forming and binding mechanism in which the intermolecular bonds were weakened, and irreversible swelling takes place by the water absorption. In particular amylase helps in gelling and amylopectin build up the polymer chains exposing large amounts of the hydroxyl groups making them hydrophilic in nature [35-37]. Due to the swelling mechanism of starch, the water in the ceramic slurry gradually decreases making the ceramic particles come closer forming a consolidated solid body.

### 2.4.1. Structure and Swelling Behaviour of Starch

Starch has been used as a processing aid in the manufacture of additives, textiles, paper, food, pharmaceuticals and building materials [5]. The properties like thickening, gelling, adhesive and film forming abilities improved the use of starch for various purposes. The optimum properties required for specific applications are obtained by the chemical, physical and enzyme treatments. These are white, dense and insoluble in nature having a different size in the range of 2-170μm. The linear polymer amylose and the branched polymer amylopectin were present in the starch in which amylopectin helps in the swelling and amylose helps in the gelation of starch in the aqueous medium. The glucose units present in the polymer chains of starch expose to the hydroxyl groups making them hydrophilic in nature (Fig. 2.2).

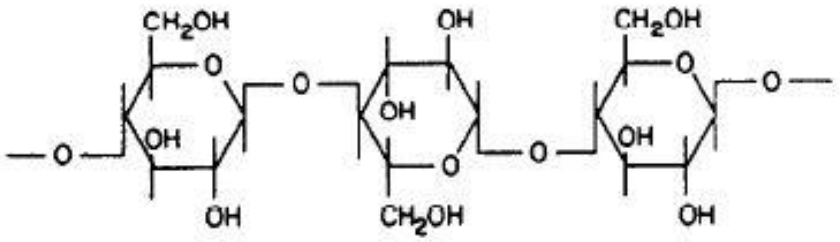


**Figure 2.2: Structure of starch granule [5]**

Starch granules are insoluble in water at room temperature making their processing easier without any effect on their granular structure. However, limited water absorption takes place in the presence of humidity leading to the slight swelling that is reversible on drying. In general the starch contains 10-17 % moisture under the normal atmospheric conditions. Rapid and irreversible swelling of starch takes place at a temperature between 50-80°C due to the breaking of intermolecular bonds holding the granules leading to the increase in the size of the granules.

Starch granules are produced by the green plants that vary in shape, i.e., spherical, oval, polygonal, elongated, etc. and size ranging between <1µm and >100µm [14]. Native starches are not soluble in water due to their semi-crystalline structure that helps in isolation of the starch granules by sedimentation, centrifugation, and filtration. Starch consists of two polysaccharides namely amylose (15-30%) and amylopectin (70-80%). Amylose is a linear molecule and amylopectin are a highly branched structure with short linear chains. These depend upon the botanical origin, the degree of maturity and growing conditions of the plant. The starch granules when heated in the presence of water or glycerol overcome the molecular forces leading to the melting of the crystalline structure called gelatinization. The onset gelation temperature is correlated to the proportion of amylopectin. The further heating of the gelatinized starch in excess water leads to the formation of paste along with the granular swelling, development of viscosity and complete disruption of the starch granules. The presence of higher amounts of amylose lowers the swelling of amylopectin reducing the pasting viscosity of the starch. Gelatinized starch recrystallizes with the loss of water binding capacity known as the starch retrogradation. High amylose content leads to the maximum rate of retrogradation.

W.Pabst et al. proposed a model for the body formation in starch consolidation casting [38]. The swelling kinetics of the starch granules with and without dispersant (0.6 Wt % related to alumina) in an 80wt% alumina suspension were studied. It has been observed that for both the cases the swelling of starch starts after 5 minutes and after 15 minutes of heating the starch granules disintegrated and transformed into a gel. It has been seen that the presence of dispersant influenced the starch swelling by the chemically interacting with the amylose and amylopectin present in starch. It has been reported that the experimental body formation time takes 33% more than the predicted time. The consolidation takes place in two stages in which initial stage is the drainage of the free water by the swelling of the starch and later the formation of the gel structure. During the second stage of consolidation, the amylose chains, and the amylopectin crystallites intrude into the interstitial pore system of the ceramic powder before the transformation of starch into a viscoelastic gel. This viscoelastic gel does not involve in the swelling of the starch.

J.L.Minatti et. al. [39] has investigated the pre-gelling and gelling characteristics of starch for starch consolidation casting. It has been observed that the gelling of starches were divided into

two stages. The first is pre-gelling of the starch where the absorption of water and swelling of the granules, forming a whitish paste takes place. The second is the gelling of the starch in which the white paste has been converted into a transparent gel. It is seen that the potato starch is suitable for the preparation of the dense ceramics using the pre-gelling of the starch since this starch contains high swelling and gel resistance. The larger size of the starch granules compared to the ceramic powder gives porosity making it difficult to obtain a dense ceramics whereas by the pre-gelling of the starch provides high mechanical resistance to the green compactness. It has been observed that the pre-gelling of starch resulted in 93% dense ceramic samples with a compressive strength of 325MPa.

The pasting and the swelling properties of the wheat starch and the starch in the presence of total amylose, free amylose, lipid complex amylose and amylopectin chain length distribution has been reported [40]. It has been observed that the increase in the total amylose content influenced the pasting properties by decreasing the peak, breakdown and final viscosities of the wheat starch. The increase in the peak and final viscosities of the starch paste has been correlated to the degree of polymerization of the amylopectin chains which is their ability to form intermolecular links with other gel components.

The relationship between the swelling and pasting properties with the structural features has been investigated using the simple and multiple regression analysis [41]. It has been observed that the swelling power and the pasting parameters depend upon the amylopectin unit chain (APC) ratio. The multiple regression analysis showed that the peak viscosity increased with low APC ratio, low amylose content, and large average granule size. The percentage of breakdown viscosity and the setback viscosity were affected by the APC ratio. Variation in the amylose content affected the total swelling of the starch. It is concluded that the fine amylopectin structure, amylose content and granule size effect on the swelling and pasting properties also related to the starch concentration in the suspension.

### 2.4.2. Burnout Behaviour of Starch

The thermogravimetric analysis (TG) of the Cassava starch showed two-stage decomposition in the temperature range 250-500$^{o}$C [28]. The initial breakdown in the temperature range 190-350$^{o}$C is attributed to the breakdown of the starch while the weight loss during the high temperature (360-500$^{o}$C) was attributed to the residual starch decomposition.

Burn out of starch is a significant step in the processing of starch consolidated ceramics. Burning of the starch occurs in the temperature range 250-500$^{o}$C leading to the generation of gaseous products [5]. The release of these gaseous products from the sample causes the development of stresses during combustion, which in turns produces cracks in the sample. Controlled burning of the starch is required to get a cracked free sample. An attempt has been made to study the rate controlled burning behavior of starch. In this process, the rate of decomposition of starch has been kept constant by varying the heating rate of the sample in the temperature range 0-1000$^{o}$C. The DTG behavior showed the presence of three peaks at 120$^{o}$C, 240$^{o}$C, and 380$^{o}$C. The study suggested that the peak at 120$^{o}$C is due to the removal of absorbed water in the starch. The peaks at 240$^{o}$C and 380$^{o}$C are due to the removal of amylose and amylopectin of the starch respectively.

The thermal analysis of starch has also been studied under two different atmospheres namely air and nitrogen [42]. DSC pattern consists of one endothermic and two exothermic peaks in the temperature range 250-350$^{o}$C, 350-420$^{o}$C and 420-550$^{o}$C respectively when observed under the oxygen atmosphere. The existence of the endothermic peak under both the atmosphere is associated with weight loss is attributed to the partial decomposition of a hydrocarbon. The exothermic change in the air atmosphere is due to the combustion of the gaseous products developed during degradation of starch.

The thermal decomposition of wheat starch was studied to establish a heating schedule to prepare a defect free porous ceramics [43]. It has been observed that 30 vol % of the reduction in weight takes place at 380$^{o}$C, and the decrease is continued till 520$^{o}$C. This indicated that the complete degradation of the organic components took place below 600$^{o}$C. Depending on this thermal analysis the slow firing is scheduled at low temperature (600$^{o}$C) for removal of organic phases followed by the sintering schedule.

K.Prabakaran et., al. [44] reported the mass loss analysis of wheat particles which involves three stages of decomposition. The three stages of decomposition took place at temperature 120-275$^{o}$C, 275-350$^{o}$C and 350-550$^{o}$C were associated with a weight loss of 22%, 50% and18% respectively. The initial decomposition is attributed to the absorbed water removal while the decomposition in later stages was attributed to the removal of hydrocarbon during the burnout

process. Since major decomposition (82%) took place below 350°C, a slow heating rate is maintained to obtain a defect-free wheat consolidated sample.

The thermal analysis of the starch consolidated green sample was studied to identify the optimal raising temperature [45, 46]. It is observed that one endothermic peak and two exothermic peaks were observed at a temperature of 70°C, 329°C, and 423°C.It has been suggested that slow heating rate should be followed to avoid the over vibrant pyrogenation during thermal removal of starch.

### 2.4.3. Rheology of Slurry

The rheological behaviour is essential for monitoring and controlling the consistency and behaviour of the slurries for casting processes like slip casting, tape casting, consolidation casting and spray drying. The slurry may contain particles in the range from granular to the colloidal size. The addition of the electrolyte and polymers affect the interparticle forces and the state of dispersion. The interparticle spacing depends upon the various factors like solid loading, the state of dispersion and particle packing. The rheological behaviour of the slurry helps to know the microstructure of the slurry system. The power law equation can describe the rheological behaviour of the slurry,

$$\tau = K\dot{\gamma}^{n} \tag{2.1}$$

$$\eta_{a} = K\dot{\gamma}^{n-1} \tag{2.2}$$

Where 'τ' is the shear stress, 'K' is the consistency factor, 'γ˙' is the shear rate, '$\eta_a$' is the apparent viscosity and 'n' is Non-Newtonian constant. The slurries for which n<1 exhibits the shear thinning behaviour where the shear stress increases with the increase in the shear rate while the viscosity decreases with the increase in the shear rate. The slurries with n>1 exhibit the shear thickening behaviour where the apparent viscosity increases and the with particle interference increase in the shear rate. This behaviour indicates a concentrated suspension with large agglomerates, concentrated and deflocculated slurries [47].

O.Lyckfeldt et al. studied the rheology of the alumina slurry in the presence of starch [5]. It has been reported that the shear thinning behaviour decreased with the increase in starch amount leading to almost Newtonian behaviour. It is seen that the modified starch contained slurry

exhibits high viscosity compared to that of the native starch. This viscosity behaviour of the modified starch is attributed to a more open structure of the granules exhibiting a high degree of water uptake. Viscosity of the slurry decreased when the alumina is replaced by the starch. This is due to the decrease in the total solid loading of the slurry as well as the exposure of the larger surface area towards the liquid phase by the submicron alumina particles. Even at a low solid loading, the viscosity increases with the increase in the starch content (45-55 vol%). The increase in viscosity is due to the water uptake by the starch granules. Thus, the free water in the slurry decreases leading to high viscosity. Hence, the viscosity of the slurry is controlled by total solid loading, total exposed surface area of the solids, the possible existence of an optimum particle packing and the water uptake of the starch. In summary, the work suggested that the viscosity should be consistent enough for mold filling without entrapped air bubbles as well as for avoiding the segregation before consolidation and significant shrinkage during consolidation and drying.

The rheological behavior of the cordierite slurries with different solid loading, starch content and type of potato starch has been studied [32]. All the slurries exhibited shear thinning behavior. The viscosity of the slurry decreased with the increased shear rate. This behavior was observed in both at high solid loading as well as high starch content in the slurry. At the low shear rate, the liquid of the slurry is entrapped between the particle flocs. On the other hand, at high shear rate, the entrapped liquid is released, and ordered structure is formed in the flow direction leading to the decrease in viscosity with an increase in shear rate. The increase in the viscosity with the increase in the starch addition is attributed to the water uptake of the starch granules decreasing the free water availability in the slurry. It had been observed that when the coarse starch powder replaced the fine starch powder, the viscosity of the slurry decreased. The high surface area of fine starch powder results in the higher water absorption of the fine starch granules. The fine starch particles are exposed a higher surface area to the liquid phase leading to an increase in the viscosity of the slurry.

Willi Pabst et al. [48] studies the shear stress - shear rate behavior of alumina slurry as a function of starch content and type of starch. The slurries were reported to exhibit shear-thinning behavior that shows an increase in shear stress with an increase in the shear rate. The thixotropic behavior increases with both at high starch content and milling time of the slurry.

The shear flow properties of the aqueous mullite starch suspension as a function of starch type has been investigated [49]. It has been observed that the viscosity decreased with the addition of the native starch to the slurry. This behavior is correlated with the decrease in the total solid loading as well as the higher affinity of the mullite particles having high surface area towards the liquid phase. The width of the particle distribution increased with the addition of the starch and thus better particle packing could also be a factor for the decrease in the viscosity. The viscosity of the slurry increased when the native starch was replaced by the modified starch that is attributed to the chemical modification and the faster water uptake due to the open starch granule structure.

### 2.4.4. Green Properties of Starch Consolidated Samples

The evolution of green densities as a function of the starch content at two solid loading has been studied [32]. It has been observed that the relative green densities showed a decreasing trend with the increase in the starch content. This behavior described the packing ability of the cordierite paste and starch together with the starch amount. The results conflict the Furnas model that says that the packing of the mixtures improves when a course particles replace a certain amount of the fine particles. This effect of packing of mixtures on the green density was due to swelling of starch during gelation.

The green properties of the starch consolidated alumina samples have been reported by Ki-Hyeon Kim et., al.[50]. It has been reported that at 60 vol % solid loading the green density increased with increase in the starch content up to 2.5vol% and then decreases with the further addition of starch. Similar behavior was observed at 56 vol % solid loading. The highest green density 55% and 64% of the theoretical density is obtained for the sample with 56 and 60 vol% solid loading respectively containing 2.5 vol% starches. The increase in density with solid loading is attributed to the closer approach of the particles with an increase in some particles in the slurry. The increase in density with starch addition is because starch forms polymer bridges by adsorption on the adjacent alumina particles. A similar trend has been observed for the flexural strength of the samples. The decrease in the strength with the increase in the starch content above 2.5 vol% was attributed to the inhomogeneous slurry mixing or due to the flocculation of the particles in the high viscous slurry.

The properties of the green alumina samples prepared by starch consolidation technique have been studied [43]. It has been reported that the green density of the samples decreases linearly with the increase in starch content in the slurry and is attributed to the presence of agglomerates in the alumina slurry. The interconnected pores and the amorphous material between the spherical particles have been observed in the microstructure of the green samples without starch. This is due to the removal of the solvent leaving the pores during the drying process while the amorphous material is the presence of polymer binder in the structure.

### 2.4.5. Sintered Properties of Starch Consolidated Samples

The preparation of high porous ceramics using the combination of the gel casting and the pore forming agent technique has been reported [43]. It has been observed that the starch addition increased the total solid loading in the suspension promoting the particle packing of the system. With the increase in the starch content from 0 to 30 vol%, the porosity increased from 67-82% while the thermal conductivity and the compressive strength decreased. The starch acting as a pore former reduces the densification without affecting the connections of the neighboring grains. However, the excess amount of starch leads to the collapse of the porous structure. The ultra-high porosity is advantageous for the heat insulation, fuel cells, and catalyst support applications.

The impact of the starch content and the sintering temperature on the mechanical, electrical and physical properties of the porous alumina ceramics prepared through starch consolidation casting has been investigated [51]. It has been observed that higher porosity could be obtained at low starch content indicating an interconnected pore, i.e., large pores connected by the small pore throats. The bulk density, apparent porosity and the pore size varied in the range 1.4 -2.05 g/cc, 46-64% and 1.79-4.28 μm respectively depending on the starch content of the suspension and the sintering temperature. Hence, the study concluded that the bulk density, apparent porosity, pore size, volume resistivity and mechanical properties of the porous alumina ceramics depend primarily on the starch content and the sintering temperature. Due to the presence of the combination properties, these porous ceramics are widely used in the thermal, electrical, bio-ceramic applications as well as the filters and gas burners.

The microstructural comparison of the porous oxide ceramics has been reported using the traditional slip casting and the starch consolidation technique [52]. It has been observed that the

maximum porosity of 50% could be obtained irrespective of the technique (TSC and SCC) and the oxide system. The porosity of the ceramics could be controlled by the amount of starch in the suspension. It has been observed that the shrinkage of the samples prepared with TSC were independent of the content and type of starch used and even the concentration of the suspension, i.e., solid loading. In the case of SCC, the shrinkage is dependent on the type of starch as well as the solid loading. The micrographs showed the presence of ceramic shell inside the pores that are formed during drying and burning of starch. The microstructure thus indicates that the properties were dependent on the interaction of the starch and the ceramic powder and were independent of the processing technique (TSC or SCC).

E.Gregorova et al. discussed the optimized preparation of the porous alumina ceramics using starch consolidation casting [13]. It has been observed that using corn starch as a pore forming agent in the concentration range 20 vol% to 50 vol% could result in a total porosity of 22% to 53%. It has been seen that the total porosity and the pore size increases whereas the density, and linear shrinkage decreases with the increase in the alumina loading in the suspension. The pore size, on the other hand, decreases with increase in the starch content where the alumina loading was constant. The paradoxical finding that the porosity increases with the increases in the alumina loading could be explained by introducing the affine limit porosity.

SCC method has been used to prepare alumina-zirconia composite ceramics with varying zirconia (10-40 wt%) and starch (10 - 50 vol %) content. The prepared composites were sintered either by partial sintering or complete matrix sintering [53]. It has been found that 70% porosity could be obtained using SCC while 50% porosity was obtained with complete matrix sintering. The pore throat sizes were mono-modal with a median diameter of 1.4 mm to 2.2 mm after complete matrix sintering while these were bimodal with the second mode of 0.1 mm to 0.2 mm during partial sintering. Hence, the partial sintering ceramic microstructure comprises of hierarchical (porosity at two levels) pore structure.

Macroporous Alumina ceramics has been prepared from aqueous $Al_2O_3$ slurries using wheat particles as gelling and pore forming agent [44]. It has been observed that wheat particles incorporated in aqueous $Al_2O_3$ slurries undergo rapid water absorption on heating leading to the formation of a strong gel. The gelled bodies did not undergo any crack and warpage during drying. The dried green bodies thus fabricated showed diametrical compressive strength in the

range 0.41–0.59 MPa and are amenable to machining operations. Pyrolytic removal of the pore-former followed by sintering at 1600°C produced $Al_2O_3$ ceramics with porosity in the 67–76.7% and diametrical compressive strength in the range 2.01–5.9 MPa. Isotropic shrinkage has been observed during sintering. Microstructural studies revealed the presence of both large (200–800 μm) and small (less than 20 μm) pores in the sintered bodies. Small pores were found to be uniformly distributed in the struts and walls of the large pores.

Starch is used as both consolidator/binder of the ceramic suspension and pore former for porous ceramic processing. Thermo-gelling behavior of aqueous suspensions of different starches namely potato, cassava, and corn has been studied by dynamic rheological testing and optical microscopy. This has been done to optimize the thermal consolidation of ceramic green bodies prepared by the starch consolidation method [54]. It has been observed that the onset temperature of gelatinization, the maximum storage modulus and the temperature for maximum storage modulus depends on the biological origin of the starch. Potato and cassava starches showed the similar values while corn starch showed the highest value. It has also been observed that with an increase in heating rate, the onset temperature of gelatinization, and the temperature for maximum storage modulus increases while the maximum storage modulus decreases. This study indicates that a low heating rate promotes the development of a stronger gel structure. It has also been reported that the presence of a dispersant, in the range used for ceramic processing, did not significantly change the viscoelastic properties of all the starches studied. The study suggested that in the context of ceramic forming by starch direct consolidation, a specific heating dwell time at the gelatinization temperature of the starch will provide green bodies with better properties.

Porous alumina ceramics was prepared using the wheat flour as the pore forming agent and body forming agent [48]. It has been observed that the pores created were not only from the swelling of the starch granules but also from the protein assisted foaming that creates foam bubbles stabilized by the starch granules during wet milling. The total porosity of 60% was obtained with 20 vol % of flour or semolina when the suspension was milled for 8 hours. The pore throat sizes were in the range of 1-2 μm when the suspension was milled for 2-3 hours while it was in the range of 20-39 μm when the suspension was milled for 8 hours.

Mechanical properties of the alumina ceramics fabricated using starch consolidation casting has been reported [50]. The samples prepared with the addition of 2.0wt% to 3.5wt% of the starch showed linear drying shrinkage of 2-3% and green density of 64% of theoretical value. Sintered density of 99.4% with a flexural strength of 247 MPa has been obtained when the samples were sintered at 1600°C for 2 hours. Uniform packing of the ceramic particles without any agglomeration or defects were observed in the micrographs of the samples with 2.5 wt% starch.

The influence of starch content and sintering temperature on the alumina bodies prepared using the starch consolidation technique has been studied [28]. The samples were dried at 60°C for 2 hours and sintered at 1200°C, 1400°C and 1600°C with a dwell time of two hours. The relative density in the range of 0.4-0.75 and open porosity in the range of 13-55% were obtained depending upon the starch content in the suspension. The microstructural studies showed that the properties of the samples primarily depend upon the starch content and the sintering temperature.

Zuzana Zivcova et., al. studied the preparation of porous alumina ceramics using different forming agents such as rice starch, lycopodium, coffee, flour, semolina and poppy seed. All the forming agents were granular (5 µm – 1 mm) and low density (1.1-1.5 g/cc) [34]. The samples were prepared using the traditional slip casting (TSC) and starch consolidation techniques (SCC). It has been observed that the all the pore formers exhibited the burning behavior between 250-550°C except the poppy seed that showed that thermal effects up to 600°C. The use of poppy seed as a pore former through the traditional slip casting was not successful because the starch needed to create pathways for gas release during pyrolysis to avoid the stress and the cracking of the samples. The study suggested that all the starch containing pore formers could be used both as pore forming and body forming agents in the starch consolidation casting.

Porous alumina ceramics has been prepared using poppy seed as pore forming agent. The advantages are large seed size (1 mm), narrow size distribution, shape (kidney-like), low density and easy availability [55]. It has been observed that bulk density of 2.50 g/cc, a total porosity of 37.6% and linear shrinkage of 14% could be achieved when the samples were sintered at 1570°C. The study also reported the formation of hierarchical pore structure when combined this technique with potato starch.

E.Gregorova et al. discussed the porosity and pore size control using the starch consolidation technique [56]. It has been found that the porosities in the range 25-50% were feasible to control while lower or higher porosities were difficult to achieve. It has been observed that the pore size could be controlled by selecting the appropriate type of starch. Among the starch types investigated, potato starch is the largest (50µm) and rice starch is the smallest (14µm) while wheat starch is the intermediate (20µm) granular size.

The influence of starch content and solid loading in the slurry on the sintered density of the porous samples has been reported [32]. It has been observed that the sintered density decreases with the increase in the starch content in the slurry. The final porosity of the samples could be correlated to the amount of starch being added to the slurry. Porous structures could be easily obtained by changing the starch content and the type of starch as well as the total solid loading of the suspension. This study suggested that the dependence of the final porosity on the starch content in the slurry enables tailored porous structure according to the application of this technique.

O.Lyckfeldt et al. has discussed the processing of porous ceramics using the starch consolidation technique [5]. It has been reported that total porosities in the range of 23-70% could be obtained by using the pore formers with spherical shape and size in the range 10-80 µm. It has been found that the pore size of the sintered samples in the range of 0.5-9.5 µm. The study suggested that the pore size could be controlled by solid loading and the starch content of the slurry. The chemically modified starch was found to give better pore size distribution of interconnected pores as compared to that of the native starch, leading to more stable properties during water processing. The major advantage of the technique was the possibility to prepare complex shapes with various mold materials and low-cost processing equipment.

### 2.4.6. Effect of Sintering Additives

The densification of alumina in the presence of $MnO_2$ and $TiO_2$ additives at a temperature of 1250$^oC$ has been studied [57]. It has been observed that the density of the samples in the absence of additives decreased from 68 to 95 % of theoretical density with the increase in sintering temperature. The densities increased from 73% to 98.7% of theoretical density in the presence of 3 wt% of $MnO_2$. Three wt% $TiO_2$ doped samples showed the similar effect as that of $MnO_2$ but at low sintering temperatures. The study suggested $TiO_2$ as a more efficient additive as compared

to that of $MnO_2$ as per densification is a concern. The densification behavior with the addition of additives is attributed to the enhanced grain growth along the grain boundaries. Beyond the certain percent of the additive, the rate of densification decreased due to the formation of the secondary phase.

The effect of $TiO_2$ on the density, microstructure and mechanical properties of alumina has been studied by M. Sathiya Kumar [58]. It has been observed that the green density of the alumina samples decreased from 58% to 53% of the theoretical density with the increase in the titania addition. At 1400°C, the density of the samples increased from 81 to 98% of theoretical density with the addition 0.2 wt% $TiO_2$ while at 1500°C the density increased from 96 to 98% with 1wt% $TiO_2$. It has been observed from the microstructure that the grain size increased from 0-0.2 wt% of $TiO_2$ and then decreased to four wt%. This behavior is due to the formation of $Al_2TiO_5$, which acts as a secondary phase reducing the grain growth by pinning effect. The flexural strength increased from 315 to 353 MPa with 0 to 0.1 wt% $TiO_2$ addition. The further increase in the $TiO_2$ content decreased the strength to 220 MPa but increased to 347 MPa when four wt% $TiO_2$ is added.

Hyoun-Ee Kim et. alhas studied the densification and mechanical properties of titanium diboride (TiB2) with silicon nitride (Si3N4) as a sintering aid [59]. It has been observed that the relative density of the pure $TiB_2$ was 90% of the theoretical density while with the addition of 2.5 wt% of $Si_3N_4$ the density increased to above 99%. It has been also observed that the grain size reduced from 7 µm to 3 µm with the addition of 2.5 wt% $Si_3N_4$. The further increase in the $Si_3N_4$ amount decreased the density slightly while the grain size remained unchanged. The flexural strength increased from 400 MPa to more than a factor of 2 with the 2.5 wt% $Si_3N_4$ addition while it decreased to 500 MPa to 5 wt% of $Si_3N_4$. This reduction in the strength behavior is attributed the formation of a large number of secondary phases at the grain boundary as well as the decrease in density of the samples.

The effect of aluminum nitride (AIN) as a sintering aid on the sintering and mechanical properties of titanium diboride has been reported [60]. It has been observed that the density increased 89 to 98% with 5 wt% addition of AIN while the densification decreased with more than 10 wt% AIN. The strength increased from 360 MPa to 650 MPa with 5 wt% AIN decreased to 480 MPa with the further addition of AIN (> 10wt %). The decrease in strength at higher AlN

addition is attributed to the density improvement in the body. Similarly, it has been observed that the fracture toughness increased from 4.5 to 6.8 MPa.m 1/2. The decrease in the strength and fracture toughness at high AlN amounts was due to the presence of unreacted AlN in the matrix.

The effect of two ($CuO + TiO_2$) or multicomponent ($CuO + TiO_2 + MgO + B_2O_3$) additives on the density, microstructure and mechanical properties of the alumina ceramics has been investigated [61]. It has been observed that theoretical density of 98.5 % was obtained with pure alumina sintered at 1550°C (dwell time of 3 hours). By the addition of diphasic additives, TD of 99.6% was obtained at 1200°C while the addition of multiphasic additives resulted in the 99.2% TD showing the complete densification at 1250°C.The addition of additives increased the densification due to the formation of low viscous liquid during sintering. It has been reported that the apparent porosity of the samples was below 0.5% for both diphasic and multiphasic additives. The toughness of the samples is increased with the addition of diphasic and multiphasic additives compared to the pure alumina at low sintering temperatures.

### 2.5. Polymeric Sponge Replica Technique (SRT)

The effect of the sintering temperatures on the strength of the alumina foams prepared by using the polymeric sponge replica technique has been studied [62]. It had been reported that the porosity of the samples decreased from 89 to 86.75%, and strength increased from 0.27MPa to 0.627MPa when the sintering temperature increased from 1400°C to 1500°C. The increase in the strength was not appreciable with the increase in the temperature of 1500°C to 1550°C, but the increase in the grain size has been observed which improved the foam strength. The further increase in the sintering temperature up to 1600°C resulted in a drastic increase in the grain size leading to the decrease in strength of the alumina foams. Hence, the present work suggested that the sintering temperature of 1550°C is required to achieve the high strength alumina foams.

Replicated silicon carbide porous ceramics has been prepared by controlling the slurry rheology [63]. It has been observed that the thixotropic behaviour of the slurry increases with the increase in the solid loading. The polymer content between the 0.05 to 0.1% showed anti-thixotropic behavior while the polymer content of 0.2% showed thixotropic behaviour indicating that with an increase in the polymer content thixotropic behaviour of the slurry increases. It has been observed that the viscosity of the slurry is increased with increase in the solid loading and the polymer content of the slurry. High viscosity slurry is required to coat the sponge struts

uniformly and to develop the SiC replica porous ceramics with uniform microstructure. The flexural strength and the densification of SiC reticulated porous ceramics has been improved with the increase in the solid loading and the polymer content. It has been concluded that the control of slurry rheology plays a significant role in the optimization of the microstructure and properties of the reticulated porous ceramics.

The preparation of the hydroxyapatite scaffolds by combining the gel casting and polymer sponge techniques has been reported by Miqin Zhang et., al.[64]. It has been found that the properties samples fabricated by the combination technique were not obtained either only by gel casing or only by polymer sponge technique. The porous scaffolds prepared by the combination technique have an open, uniform and interconnected porous structure. These scaffolds have a pore size in the range of 200-400 mm, the compressive strength of 5 MPa and compressive modulus of 8 GPa. The macroporous structure of the produced scaffold is the replicate of polymer sponge technique by which the pore size and shape were controllable and complex structures could be fabricated. Since the scaffolds were formed by the in-situ polymerization, the aggregation of the slurry at the bottom due to the gravitational force can be prevented leading to a homogenous microstructure. It has been suggested that the combination technique could be applied to the bioceramics with enhanced mechanical strength for load bearing tissue engineering.

Xiumin Yao et. al studied the effect of the recoating slurry viscosity on the properties of the reticulated porous SiC ceramics [65]. It has been observed that the high viscosity slurry with the thixotropic loop is required for the recoating of the polymeric sponge. The increase in viscosity due to the increase in solid loading leads to an increase in loading of SiC replicated porous ceramics results in a decrease in cell size and an increase in strut thickness. The decrease in the cell size and increase in the strut thickness attributes to increase in the solid loading. The compressive strength of the samples increased from 0.78MPa to 1.59MPa as the recoating viscosity increased from 0.07Pa.s to 1.44Pa.s. It has been seen that the microstructure of the samples contains both large pores and the small pores. The small pores were caused by the sintering while the large pores were due to the entrapped air bubbles. The roller method used to remove the excess slurry removes the part of the air bubbles. The excess slurry removal by the

centrifugal technique could not remove the air bubbles during the process leading to increased porosity after recoating.

Hydroxyapatite porous ceramics has been prepared using polymeric sponge method reported [15]. The porosity of the samples was found to be 0.2-1.0 mm in the micropores range and 100-500 mm in the macropores range. The compressive strength of the samples increased from 1.8 MPa to 10.5 MPa with the decrease in the porosity from 59.8% to 34.3%. The increase in the compressive strength has been attributed to the fast sintering schedule adopted in the study leading to an increase in the apparent density and crystallinity of the samples. It has also been reported that prolonged stirring the slurry resulted in the high compressive strength of the samples due to the better homogeneity in the slurry.

The improvement in the strength of reticulated porous ceramics by vacuum degassing has been reported [6]. Air bubbles were found to affect the viscosity of the slurry during impregnation. Vacuum degassing stage prior to impregnation has been introduced to remove air bubbles from the slurry. It has been observed that this step was effective in removing the defects in the strut and increase the flexural strength of the sample from 2.34 to 3.18MPa.

# Chapter 3 Objectives

A schematic diagram indicating microstructural changes (as understand from the literatures) of porous ceramics fabricated by starch consolidation casting (SCC), sponge replica technique (SRT) and combination of SSC and SRT is provided for ready reference in Fig. 3.1.

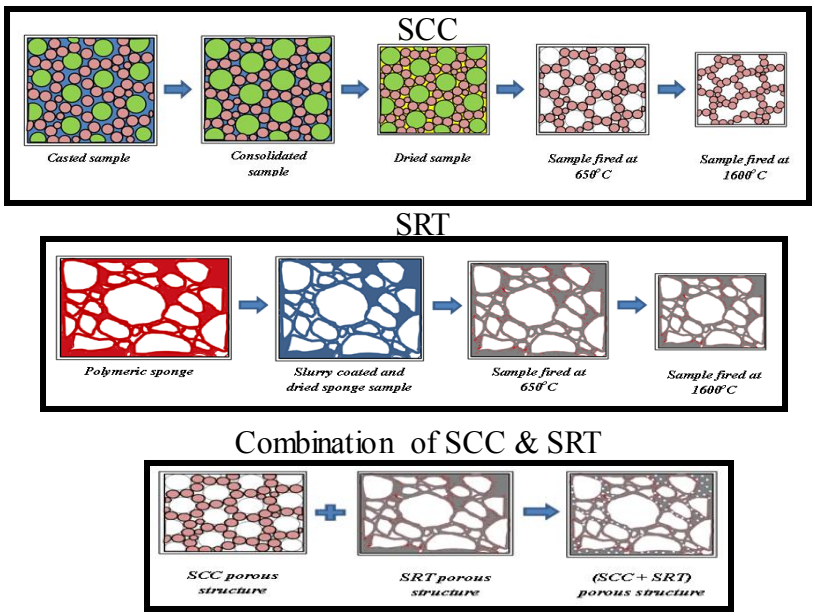


**Figure 3.1: Schematic diagram indicating the microstructural changes during fabrication of porous ceramics following techniques adopted in the present study.**

The extract from the literature that acts as motivators of the present work are as follows:

1. Porous ceramics having porosity 20-70% with a pore size in the range of 2-200µm is possible by controlling the process parameters in SSC technique.
2. Porous ceramics having porosity 40-90% with a pore size in the range of 200µm-3mm is possible by controlling the process parameters in SRT technique.
3. The strength of porous ceramics decreases exponentially with the increase in porosity (or decrease in density) of the sample.
4. $TiO_2$ has been well studied as a sintering additive for alumina ceramics.

The factors affecting the porosity of the ceramics fabricated by starch consolidation casting (SCC) technique are solid loading of the slurry, rheology of the slurry. Physical properties of the starch (including swelling and hydration behaviour, the amount of starch present in the slurry) also affect the porous sample. Further, the porosity and strength of the ceramics could also be controlled by the extent of densification of final ceramics (sintering temperature). For examples

samples (prepared from the same slurry) sintered at low temperature are expected to have high porosity and low strength or vice versa. The decrease in porosity with an increase in sintering temperature (And the use of sintering additive) could be compensated by an increase in pore former (or lowering the sintering temperature). Porosity in the porous ceramics could be developed by different ways. Sintering at high temperature with more amount of pore former could produce an equivalent porosity in the samples while sintered at a low temperature with less amount or pore former. The same amount of porosity could also be developed while sintering at a low temperature in a sample prepared with the addition of sintering additives keeping pore former constant.

On the other hand, solid loading or slurry rheology has been identified as the important parameters for sponge replica technique (SRT). Moreover, one could prepare hierarchical (two different sized pore combination) porous ceramics by SRT techniques using a starch containing slurry. The detailed work dealing with porous structure developed in ceramics fabricated by a combination of SCC and SRT is hardly available in the literature.

In view of the above, objectives of the present study are as follows:

1. Theoretical prediction of porosity of SCC fabricated samples.
2. Processing and fabrication of the porous alumina ceramics using SCC.
3. Study of the effect of alumina loading, starch content and type of starch on the properties of the porous ceramics prepared by SSC technique and validation of the theoretical model.
4. Study the effect of sintering additive ($TiO_2$) on the strength and porosity of porous ceramic.
5. Processing and characterization of the porous alumina samples using SRT.
6. Fabrication of hierarchical porous alumina ceramics by the combination of SRT and SCC.
7. Finally development of porous alumina ceramics with wide porosity range (10-90%).

# Chapter 4 Experimental Procedure

### 4.1. Optimization of Dispersant for Preparation of Stable $Al_2O_3$ Slurry

Darvan C has been used as dispersant in the present study. Darvan C has been used to prepare the aqueous alumina slurry (with 25 vol. % $Al_2O_3$ loading). The concentration of Darvan C has been varied in the range 0.1 to 0.8wt% (based on the active matter) of dry alumina powder. The stability of the slurry has been evaluated by measuring the viscosity and the sedimentation height measurement. The sediment height has been measured after 24 hours of settling.

### 4.2. Processing of Porous Alumina Ceramics

Porous alumina ceramic samples have prepared by three different techniques. These are Starch Consolidation Casting (SCC) using corn, arrowroot and fine flour as the pore formers, Sponge Replica Technique (SRT) using polymer sponge as the template and combination of the SCC and SRT methods. The fabrication of porous alumina ceramics using the three techniques is given in Fig 4.1.

#### 4.2.1. Starch Consolidation Casting (SCC)

An aqueous slurry of alumina has been prepared using 0.3wt% Darvan C (based on the active matter) at different solid loading (30, 35, 40, 45vol %). Different amount of starch (i.e., corn starch, arrowroot and fine flour) in the range 1-50 vol% (calculated on the basis of alumina loading) has been added to the alumina slurry. The slurry has been pot milled in polyethylene bottles for one hour using alumina grinding media. The rheological behavior of the stable slurries has been studied at room temperature.

The stabilized slurry has been cast in preheated cylindrical metal molds (20mm x 20mm). The molds were lubricated with grease for easy demolding. The cast samples were kept at 90$^oC$ for 2 hours for hydration of starch and setting of the gel. After setting, the casts were de-molded and dried at room temperature for 24 hours for development of sufficient green strength. The dried samples have been heated at 1oC/min up to 850$^oC$ (with a dwell time of 1 hour) to burn out the pore former. Subsequently, the samples were heated at 3$^oC$/min to the desired sintering temperature (1300$^oC$-1600$^oC$) with a soaking time of 2 hours. The sintered samples have been characterized by porosity, pore size distribution, strength, and microstructure.

#### 4.2.2. Sponge Replica Technique (SRT)

Alumina slurry containing different alumina content in the range 20-35vol% has been prepared by adding 0.3wt% Darvan C as a dispersant. Poly Vinyl Alcohol (PVA) in the range, 1-5% has

been added to the slurry as the binder to maintain the viscosity of the slurry. Sponge samples (2 x 2 x 2 cm) were impregnated with the as prepared alumina slurry, and the soaked sponge samples are dried at 90°C for 12 hours. The samples have been sintered in the temperature range 1400-1600°C. The firing schedule has been maintained as that of the SCC at two different temperatures. The sintered samples have been characterized by porosity, pore size distribution, strength and microstructure.

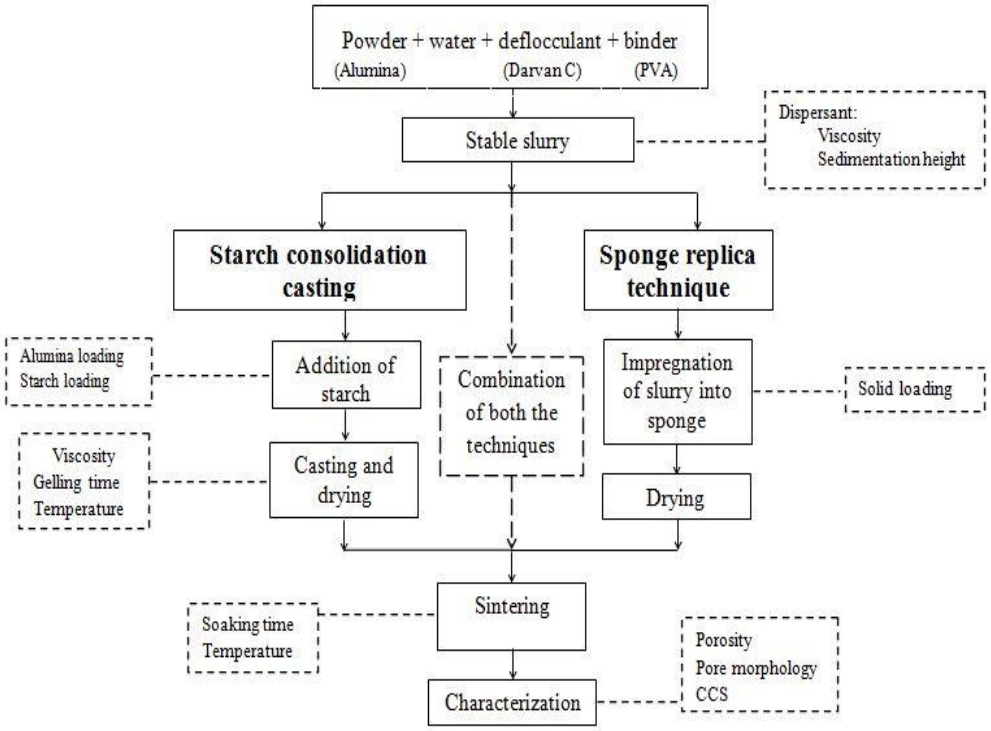


**Figure 4.1: Flowchart of sample preparation adopted in the present study**

### 4.2.3. Combination of SCC and SRT

Alumina slurry containing 20 vol. % of $Al_2O_3$ has been prepared by adding 0.3 wt. % Darvan C as a dispersant and 3 wt. % of PVA as the binder. Different amounts of corn starch (30 and 40vol. %) calculated on the basis of alumina loading were added to the slurry. Similar drying and firing schedule is maintained as that of the SRT at two different temperatures (1400 and 1600°C). The sintered samples are characterized by porosity, pore size distribution, strength, and microstructure.

## 4.3. Characterizations

### 4.3.1. Study of Swelling Behaviour of Starch

A small quantity of starch powder was taken in a 50ml measuring cylinder, and 45ml of deionized water was added to it. The setup has been placed in a preheated air oven. This experiment has been conducted at 80°C and 90°C.The swelling of the starch has been recorded after every 15mins. The degree of swelling of starch corresponds to the percentage volume increase of starch observed as a function of time at two different temperatures. The physical appearance of the sample before and after swelling has been shown in the Fig. 4.2.

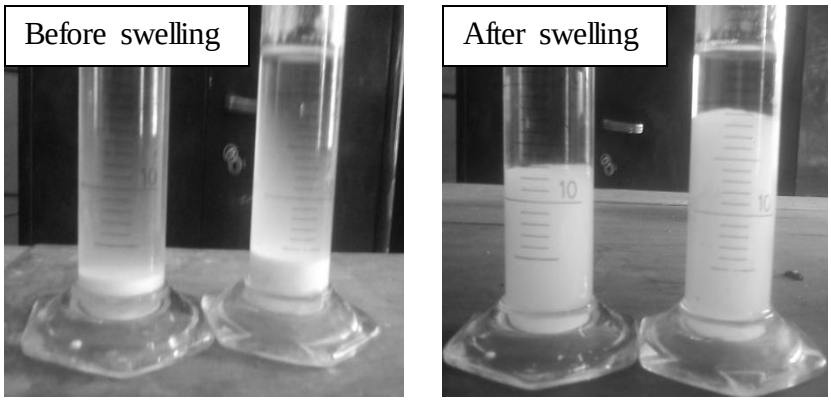


**Figure 4.2: Physical appearance of the sample before and after swelling**

### 4.3.2. Rheology Study

The rheological behavior of the stable slurries has been studied using the Anton Parr Rheometer. The measurements were carried out with an increasing shear rate (1-100 $s^{-1}$) at 25°C. The different rheological properties such as viscosity, shear stress and non-Newtonian index of the slurry has been studied.

### 4.3.3. Porosity Measurement

The porosity of the prepared alumina samples has been measured by Archimedes principle. Dry weights of the samples were taken, and then the samples were kept in a beaker filled with water. The system was then placed in a vacuum desiccator for about one hour under vacuum. The suspended and soaked weight of the samples was recorded. Porosity and density of the samples have been calculated using the formulae given below

$$Apparent\ Porosity = \frac{Soaked\ Weight - Dry\ Weight}{Soaked\ Weight - Suspended\ Weight} \quad (4.1)$$

$$Bulk\ Density = \frac{Dry\ Weight\ X\ Density\ of\ Water}{Soaked\ Weight - Suspended\ Weight} \quad (4.2)$$

$$Relative\ Density = \frac{Bulk\ Density}{Theoretical\ Density}\ X\ 100 \quad (4.3)$$

The theoretical density of $Al_2O_3$ has been taken as 3.98 gm/cc in the present study.

### 4.3.4. Compressive Strength of the Samples

The binding behavior of starch on $Al_2O_3$ has been studied from the green strength measurement of the samples in the compression mode. The compressive strength of the sample (both green and sintered) was measured using Universal Testing Machine (Tinius Olsen HK 10S). The samples were kept in the two compression platen and broken in compression at a cross head speed of 0.5mm/min. The load cell was 1 KN.

### 4.3.5. Microstructural Study

High resolution scanning electron microscopy (FESEM) is a typical electron microscope by which images are formed by simply scanning it with a beam of electrons. The secondary electrons (SE), backscattered electrons (BSE) as well as the characteristic X-rays interact with the surface atoms and provide the relevant information about the samples microstructure. The microstructure of the porous alumina samples has been studied using scanning electron microscope (Nova Nano SEM - 450). The samples were gold coated to avoid charging.

# Chapter 5 Theoretical Prediction of Porosity in SCC Samples

Let us assume water based alumina slurry prepared with '$V_{Alumina}$' $Al_2O_3$ loading (two component basis). Slurry then consists of $V_{Alumina}$ volume percent of alumina and $V_{Water}$ volume percentage of water. $V_A$ is the volume of alumina and $V_W$ is the volume of water in the slurry. The slurry contains the following

$$V_A = \frac{V_{Alumina}}{V_{Alumina} + V_{water}} * 100 \quad (5.1)$$

$$V_W = \frac{V_{water}}{V_{Alumina} + V_{water}} * 100 \quad (5.2)$$

Starch content in the slurry ($V_s$) is calculated based on the percent alumina (two component basis) in the slurry.

$$V_S = \frac{V_{Starch}}{V_{Starch} + V_{Alumina}} * 100 \quad (5.3)$$

The composition of the slurry (three component basis) is as follows

$$\text{Alumina} = V'_A = \frac{V_A}{100 + \frac{V_S V_A}{100 - V_S}} * 100 \quad (5.4)$$

$$\text{Starch} = V'_S = \frac{\frac{V_S V_A}{100 - V_S}}{100 + \frac{V_S V_A}{100 - V_S}} * 100 \quad (5.5)$$

$$\text{Water} = V'_W = \frac{100 - V_A}{100 + \frac{V_S V_A}{100 - V_S}} * 100 \quad (5.6)$$

During consolidation, starch present in the slurry swells. The percent swelling of the starch 'a' is measured by the volume changes upon swelling of starch. It is worthy to note that the volume increase of the starch on swelling is equal to the volume of water required for swelling.

$$\text{Increase in the volume of starch on swelling} = \frac{a}{100} * V'_S \quad (5.7)$$

$$\text{Volume of starch on swelling} = V''_S = V'_S + \left(\frac{a}{100} * V'_S\right) \quad (5.8)$$

$$\text{Volume of water remaining in the slurry} = V''_W = V'_W - \left(\frac{a}{100} * V'_S\right) \quad (5.9)$$

The model assumes that the swelled starch does not undergo any shrinkage during drying i.e., it retains its swelled structure in the dry body. Free water ($V''_W$) removed during drying is associated with i) dry shrinkage of the body ($V_{Sd}$) and ii) interparticle porosity (packing porosity) in the dried body (green body). Thus the green (dried) body will consists of i) alumina ($V'_A$), ii) volume of swelled starch ($V''_S$) and iii) green (dried) porosity. The later part will be equal to $V''_W - V_{Sd}$. These three components when calculated on percentage basis will result as follows:

$$V'''_A = \frac{V'_A}{100 - V_{Sd}} * 100 \quad (5.10)$$

$$V'''_S = \frac{V'_S + (\frac{a * V'_S}{100})}{100 - V_{Sd}} * 100 \quad (5.11)$$

$$V'''_{gP} = \frac{V'_W - (\frac{a * V'_S}{100}) - V_{Sd}}{100 - V_{Sd}} * 100 \quad (5.12)$$

Thus, $V'''_{gP}$, the green porosity (on drying) of the starch consolidated body could be well predicted by the above equation (5.12).

During firing, the starch burns out and produces porosity. It undergoes volume shrinkage ($V_{Fd}$) due to densification. Thus a sintered starch consolidated body will have i) alumina ($V'''_A$) and ii) porosity (sintered porosity). The sintered pore volume will be equal to the volume of green porosity ($V'''_{gP}$) plus volume of swelled starch (pore former porosity) ($V'''_S$) minus the volume shrinkage ($V_{Fd}$). These two components calculated on percentage basis will result as follows:

$$Alumina = \frac{V'''_A}{100 - V_{Fd}} * 100 \quad (5.13)$$

$$Pores = V'''_{fP} = \frac{V'''_S + V'''_{gP} - V_{Fd}}{100 - V_{Fd}} * 100 \quad (5.14)$$

Thus the total porosity of the sample could be predicted by equation (5.14).

# Chapter 6 Results and Discussion

## 6.1. Raw Material Characterization

### 6.1.1. Particle Size Distribution of Alumina

The particle size distribution of the as received calcined alumina powder used in the present study has been shown in the Fig.6.1. The particle size of the alumina showed a tri-modal distribution with a particle size varying from 0.7 to 800µm. Three distinct size particles ranges 200-800µm, 20-200µm and 0.7-20µm could be observed from the figure. A detailed analysis of the particle size distribution pattern showed 74% particles are of 0.7-20 µm, 10% particles are of 20-200µm, and particles of 200-800µm size are only 16%.

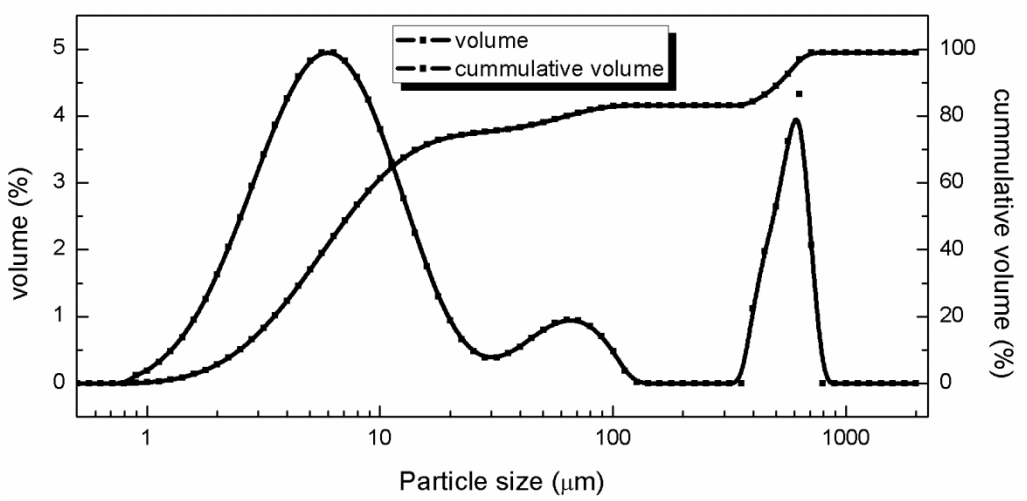


**Figure 6.1: Particle size distribution of alumina powder**

### 6.1.2. Morphology of Alumina and Starch Powder

Morphology of alumina, as well as starch powders used in the present study, has been shown in Fig. 6.2. Alumina Powders [Fig. 6.2 (a)] showed the presence of large agglomerates in the matrix of small particles and were on the same line as observed in particle size distribution. The shape of the powder was found to be irregular. Corn powder [Fig. 6.2 (b)] showed the presence of both small and large size particles. The particles size measured from the image analysis was found to be in the range of 6-18µm. It could be observed that the particles are of irregular in shape. Arrowroot particles [Fig. 6.2 (c)] showed that the particle size ranges 11-32µm. The particles are also irregular in shape. Fine flour particles [Fig. 6.2 (d)] are spherical in shape and have the size distribution in the range of 3-13µm.

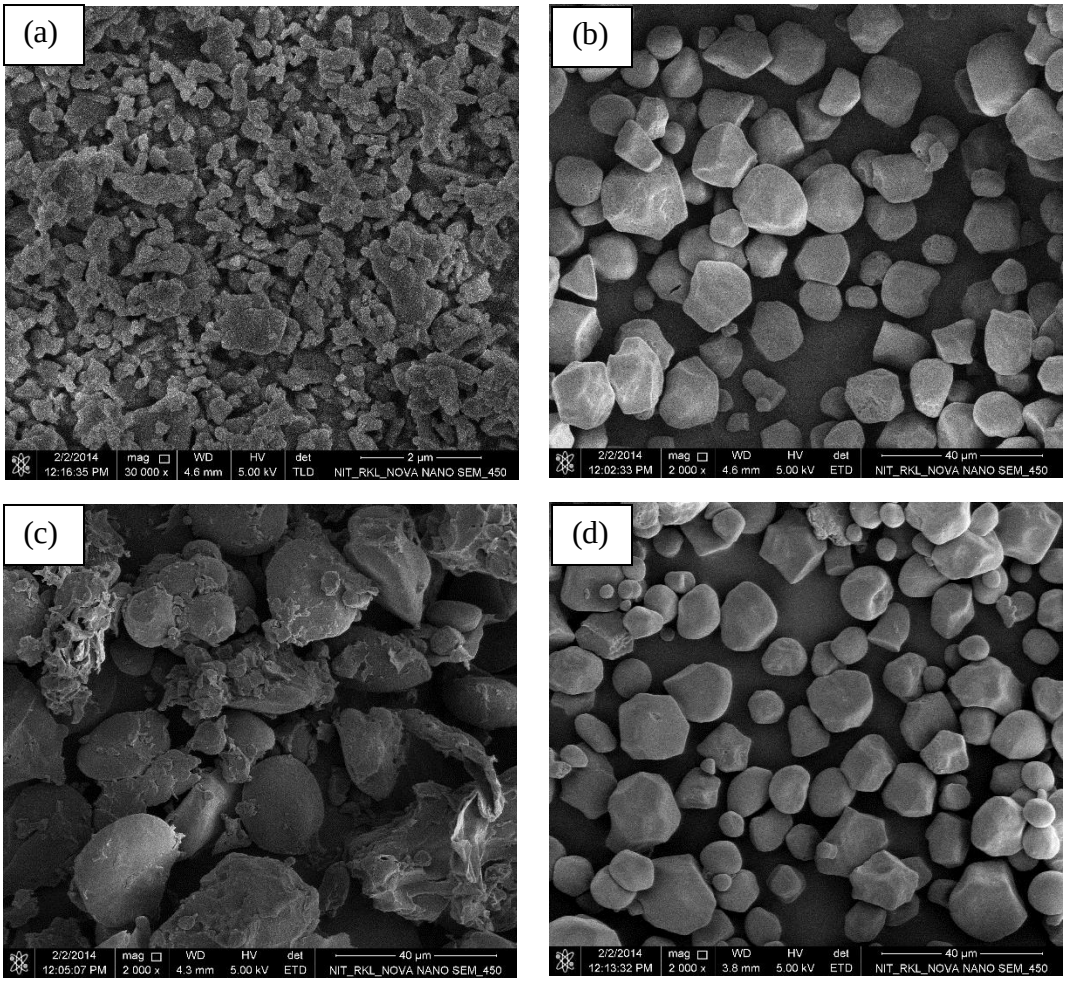


**Figure 6.2: Morphology of (a) Alumina, (b) Corn, (c) Arrowroot and (d) Fine flour powder**

### 6.1.3. Burn out Behavior of Different Starch

In the present study, starch has been used as a consolidator, binder, and pore former. Complete removal of the starch during firing is an important step to producing crack-free porous ceramics fabricated by starch consolidation. Thus, the study of burning behavior of the starch is an important step to prepare porous ceramics by this technique. The thermal decomposition behaviors of the different types of starch used were studied by DSC-TG (Fig.6.3). The decomposition behavior of corn [Fig.6.3(a)] showed the presence of three endothermic peaks at low temperatures (83$^{o}$C, 268$^{o}$C and 294$^{o}$C), two exothermic peaks at 322$^{o}$C and 465$^{o}$C in the DSC plot. All the peaks observed in the DSC curve are associated with weight loss that could be seen from TG curve. The endothermic peak at 83$^{o}$C is due to the removal of absorbed moisture in the corn. The endothermic peaks in the temperature zone of 250-350$^{o}$C are associated with the non-oxidation process and are attributed to the breakdown of starch. The exothermic peaks in the

temperature zone of 350-500°C are associated with oxidation process and are attributed to the combustion of gaseous products generated during degradation [42]. Thus in the present study small endothermic peaks at 268°C and 294°C are due to the breakdown of starch present in corn. The exothermic peaks at 322°C and 465°C are attributed to the combustion of the hydrocarbons present in the corn.

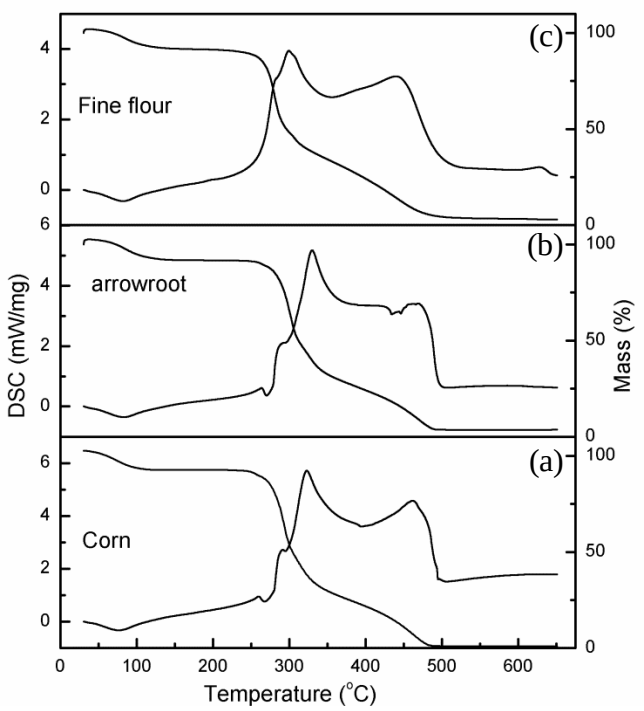


**Figure 6.3: DSC/TG pattern of starches used in the present study (a) Corn, (b) Arrowroot and (c) Fine flour.**

The burn out behaviour of the arrowroot and fine flour are shown in the Fig [6.3 (b) and (c)] respectively. From Fig.6.3 (b), it could be observed that similar to corn starch arrowroot have three endothermic peaks, two exothermic peaks indicating the burnout between 200°C and 650°C. Whereas Fig.6.3(c) shows that fine flour burn out behaviour has one endothermic peak and three exothermic peaks associated with the weight loss. This is attributed to decomposition and combustion as discussed. TG analysis showed negligible weight retention above 650°C in all the starches studied.

## 6.2. Stabilization of Alumina Slurry

Any slurry processing technique requires the dispersion of ceramic powder in the aqueous medium. The stable slurry is required in order to avoid segregation and hence density

inhomogeneity in the cast body [31]. Hence, the optimum amount of dispersant for a particular ceramic powder is required to obtain defect-free and high-quality products. Dispersant stabilizes ceramic slurry through electrostatic/ electrosteric stabilization mechanism [16].

Organic and inorganic dispersants adsorbed on the surface of the powder increase the repulsive interaction between the powder particles, either by increasing the particle charge or by building up a steric barrier between the particles. Darvan C has been used as deflocculant in the present study. Darvan C absorbs on alumina particles develops negative surface charge on the surface of the alumina particle resulting strong repulsion between the particles. [11].

### 6.2.1. Effect of Dispersant on the Viscosity of the Slurry

The effect of dispersant (Darvan C) on the viscosity of alumina slurry is shown in Fig.6.4. Darvan C concentration was varied based on active matter content in the polymer solution per dry alumina powder.

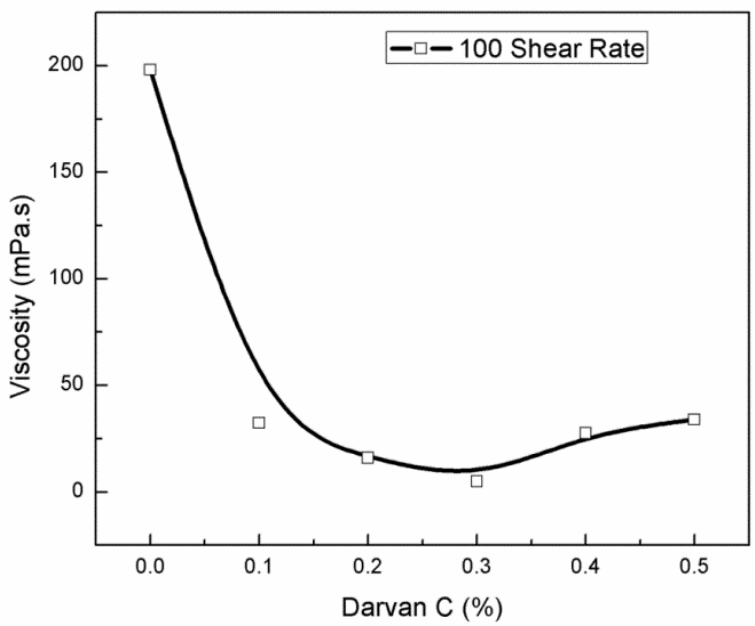


**Figure 6.4: Effect of dispersant (Darvan C) on the viscosity of alumina slurry**

It could be observed that the viscosity of the slurry decreases from 0.1 to 0.3 wt. % Darvan C and then increases from 0.3 to 0.8 wt. % of the Darvan C. The decrease in the viscosity is correlated with the increase in surface charge of the particle due to increased adsorption leading to enhanced repulsion between the particles. The rise in viscosity with high deflocculant content (typically greater than 0.3%) is due to an excess of the dispersant.

### 6.2.2. Effect of Dispersant on the Sedimentation Height

Slurry stability was evaluated by measuring the sediment height of powder from the slurry as a function of time and dispersant concentration. The sedimentation height as a function of time is represented in the Fig.6.5 (a). It could be seen that the sedimentation height increases with the time due to higher settling of particles.

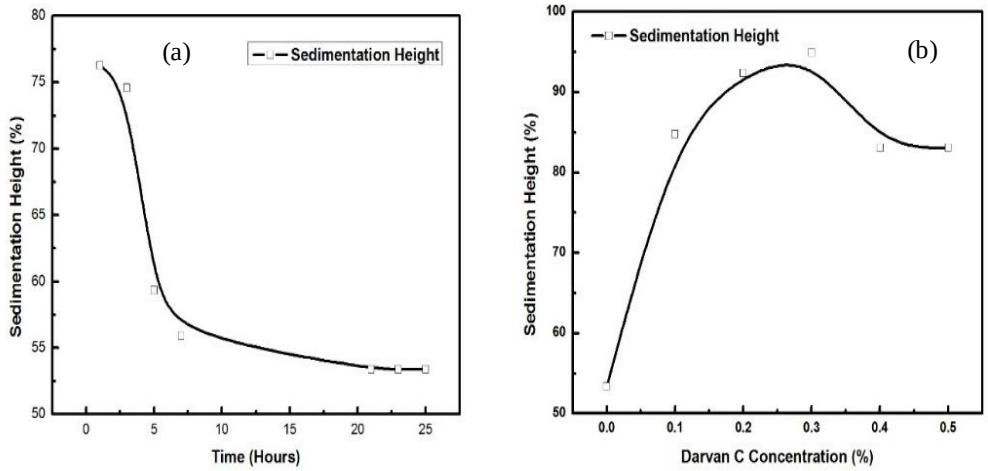


**Figure 6.5: Sedimentation height of alumina slurry (a) as a function of time slurry prepared with 0% electrolyte and (b) as a function of electrolyte content measured after 24 hours.**

There is no significant change in the height of the sediment after 24 hours. Figure 6.5(b) represents the change in the sedimentation height of alumina as a function of Darvan C after 24 hours. The sediment height decreases up to 0.3wt% of Darvan C addition followed by an increase in the sediment height in the range 0.3 to 0.8 wt% Darvan C. The minimum settling occurred was observed at 0.3wt% and is correlated with the stability of the slurry. As the dispersion content in the slurry increases the repulsive force between the particle increases. This increase in repulsive force is attributed to the decrease in the sedimentation height. The increase in the sedimentation height at high Darvan C amount (> 3%) is due to the overcrowding effect and the overlapping of the electric double layer. This resultant increase of the Van der Waal's attractive forces causes an increase of the sedimentation height of the slurry.

## 6.3. Starch Consolidation Casting

### 6.3.1. Swelling Behavior of Different Starch

Starch contains amylose (15-30 %) and amylopectin (70-85%) [8], among them amylopectin molecules are crystalline in nature and dictate the crystallinity of the starch. Amylopectin in contact with water undergoes hydration at a temperature above 70°C, due to the penetration of water in the amylopectin structure. This hydration reaction results in an increase in the volume of amylopectin. Hence, starch undergoes swelling when heated with water. This hydration reaction depends on the temperature of the water- starch system. The rate of the reaction increases with increase in temperature. The amount of swelling depends on the crystallinity of the starch and hence the amylopectin present in it. The amount of amylopectin present in different starch varies with the type and its biological origin [67]. Thus, the amount of swelling is likely to be different in the various type of starches.

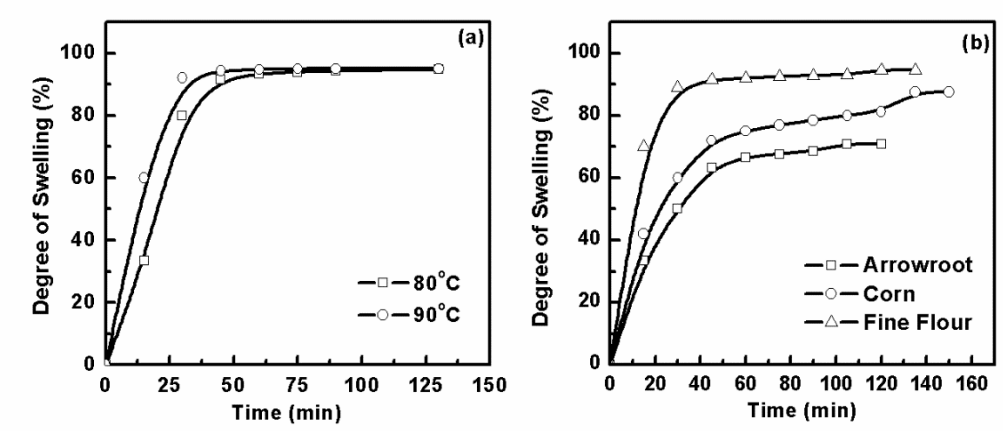


**Figure 6.6: Degree of swelling of corn starch as a function of time (a) effect of swelling temperature and (b) effect of type of starch.**

The swelling behavior of starch as a function of time, temperature, and type (biological origin) has been provided in Fig.6.6. While Fig. 6.6(a) shows the swelling behavior of corn starch as a function of time and temperature and 6.6(b) shows the swelling behavior as a function of starch type. It could be seen from the Fig.6.6 (a) that corn starch showed a maximum swelling of 87%. It could also be observed that the starch undergoes a rapid swelling during initial period whereas it slows down as the time increases. The volume expansion of the starch on heating was due to the water uptake by amylopectin molecules present in starch [41]. This process also involves the

destruction of amylopectin crystalline structure and formation of gel [67].The swelling characteristics and the maximum amount of swelling (total swelling) were found to be independent of consolidation temperature. The only difference was observed lies with the time required for complete swelling. It was found to increase with the decrease in swelling temperature. This is because of the swelling kinetics where the rate of swelling is more at high temperature than that at low temperatures.

The amount of swelling and the time for complete swelling was found to vary with the source (type) of starch [Fig.6.6 (b)]. The complete hydration for arrowroot, corn starch and fine flour at 90$^{o}$C was observed after 120 min, 140 min and 160 min respectively with a corresponding swelling of 65%, 87% and 95%. The difference in the swelling behaviour is correlated with the amylopectin contents in the starch studied [41].

### 6.3.2. Rheology of the Slurry

The rheological study plays a vital role to understand the slurry processing. Starch containing ceramic slurry exhibits a thixotropic hysteresis loop in shear stress and shear rate behavior [10]. The presence of hysteresis loop indicates shear thinning behavior [32]. The rheological behaviour of the alumina slurry (loading 35%) with different amounts (1-30 vol. %) of the corn starch is shown in Fig. 6.7(a). The slurries exhibited shear thinning behaviour as indicated by the presence of distinct hysteresis loop in the shear stress - shear rate curve. It could be observed that the hysteresis loop decreases with a decrease in corn content in the slurry. The increase in the hysteresis loop indicates the formation of particle-binder-particle interaction leading to the transformation of the slurry to the viscoelastic mass.

Non-Newtonian index of the slurry has been calculated using the power law model equation 2.2 [68]. The shear thinning index values have been found to be in the range 0.35-0.79 (Table VI.III). The ‘n’ value indicates that all the slurries investigated in this study showed Non-Newtonian behavior. Figure 6.7(c) indicates the viscosity as a function of solid loading as well as the corn addition in the slurry. The increase in viscosity either with an increase in alumina loading or increase in starch addition is due to increase in particle agglomeration in the slurry [10].

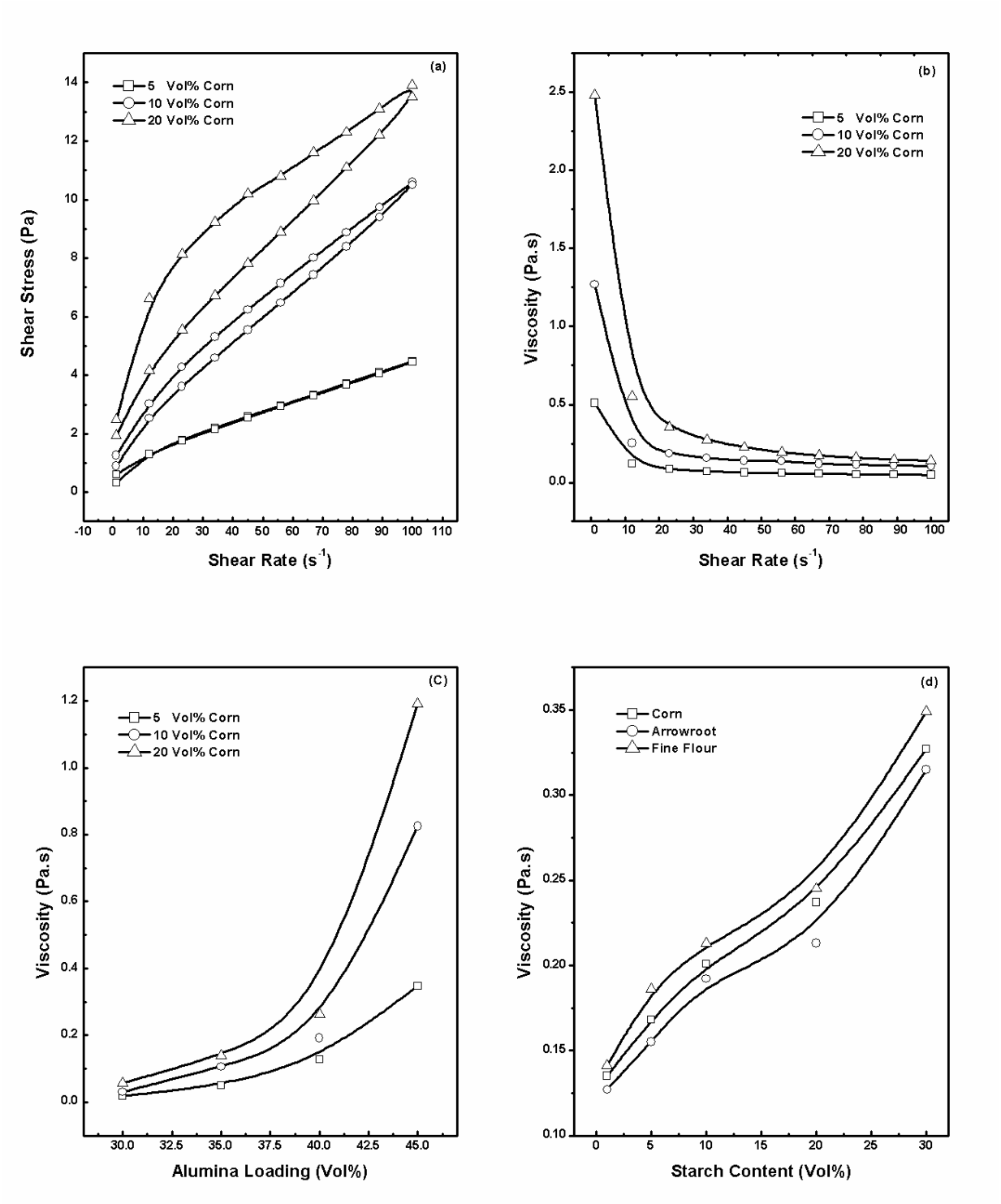


**Figure 6.7: Rheological behavior of starch containing $Al_2O_3$ slurry a) shear stress shear rate behavior, b) viscosity shear rate behavior, c) effect of alumina loading on the viscosity of the slurry and d) effect of different types of starch content.**

**Table VI.III: Consistency factor (k) and Non-Newtonian Index (n) of alumina slurry studied.**

| Alumina Loading (Vol. %) | Corn Starch Content (Vol. %) | Consistency Factor (K) | Non-Newtonian Index (n) |
|---|---|---|---|
| 30 | 20 | 0.96 | 0.3734 |
| | 30 | 0.57 | 0.3854 |
| | 40 | 0.64 | 0.5962 |
| | 50 | 0.72 | 0.7952 |
| 35 | 1 | 0.60 | 0.5766 |
| | 5 | 0.71 | 0.4917 |
| | 10 | 1.04 | 0.4507 |
| | 20 | 1.49 | 0.3742 |
| | 30 | 1.50 | 0.3979 |
| | 40 | 1.62 | 0.6076 |
| 40 | 1 | 1.19 | 0.4371 |
| | 5 | 1.28 | 0.4242 |
| | 10 | 1.60 | 0.4015 |
| | 20 | 1.71 | 0.3683 |
| | 30 | 2.19 | 0.4515 |
| 45 | 1 | 1.42 | 0.3800 |
| | 5 | 1.75 | 0.3537 |
| | 10 | 2.27 | 0.2812 |
| | 20 | 2.63 | 0.5230 |

The viscosity of the slurry as a function of shear rate at different corn starch content is plotted in the Fig. 6.7(b). It could be seen that the viscosity decreases with the increase in the shear rate. This behavior again indicates shear thinning characteristics of the slurry. Viscosity also increases with the increase in the corn content of the slurry. This could be correlated to the powder agglomeration in the slurry. At high solid loading slurry, the viscosity was found to be strongly dependent on shear rate as compared to that observed in slurry prepared with low solid loading. Figure 6.7(d) represents the effect of starch content and type of starch on the viscosity of the slurry (loading 40%). The viscosity of the slurry is increasing with the increase in the starch addition irrespective of the starch type and could be explained in terms of solid loading in the same line as discussed earlier. The viscosity is found to change the type of the starch for a fixed amount of starch content. It could be seen that the slurries prepared with fine flour have the highest viscosity whereas, slurries prepared with arrowroot showed the lowest viscosity. Slurries prepared with corn starch showed an intermediate behavior. It could be seen from Fig 6.2 that

fine flour showed the smallest particle size while arrowroot showed the largest particle size. Corn has the intermediate particle size. The increase in the viscosity is attributed to the decrease in the particle size of the starch in the same line as reported earlier [32].

### 6.3.3. Gelation Behaviour of Corn Starch

The effect of temperature on the viscosity of an alumina (25 vol%) slurry containing corn starch (30 vol% with respect to $Al_2O_3$) has been shown in Fig 6.8. The viscosity was found to decrease in the temperature range 40-55°C then increases in the temperature range 55-65°C. This experiment was conducted to ascertain the temperature at which the corn starch undergoes polymerization and gelling resulting in setting off the cast.

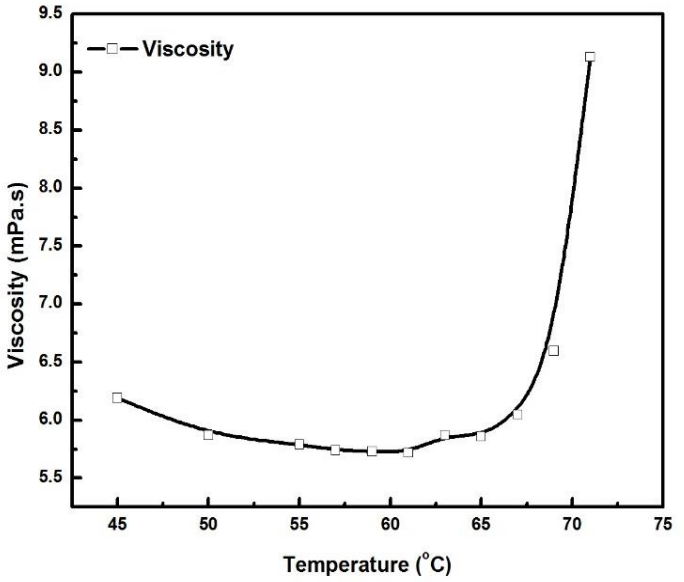


**Figure 6.8: Gelling behaviour of corn starch.**

Fig. 6.8 shows that viscosity is 6.15 mPa.s at 45°C, and it did not change appreciably till 67°C. The viscosity increases to 6.6 mPa.s at 69°C and 9.2 mPa.s at 71°C. The sudden increase in viscosity between 69 -71°C implies the gelling of the starch takes place between 69-71°C and for proper setting and hardening of the cast, the cast needs to be dried at 71°C or higher.

### 6.3.4. Compositional Study

Viscosity plays a major role in the mixing and casting properties of the starch-containing slurry. It has been observed that to obtain defect-free consolidated samples, the viscosity of the slurry

has to be maintained in the range of 0.05-1.19 Pa.s. The viscosity of alumina-water-corn system can be tailored by altering the ratio of these three components. An attempt has been made to find the optimum composition range in the three component systems of starch, water, and alumina. So as the slurry prepared with the composition would have a viscosity in the above range and has been presented in a ternary diagram Fig. 6.9. Figure 6.9 shows that to have the slurry viscosity in the range 0.05-1.19 Pa.s, the alumina and starch content of the slurry should be in the range of 23-44 vol% and 0.3-25 vol% respectively.

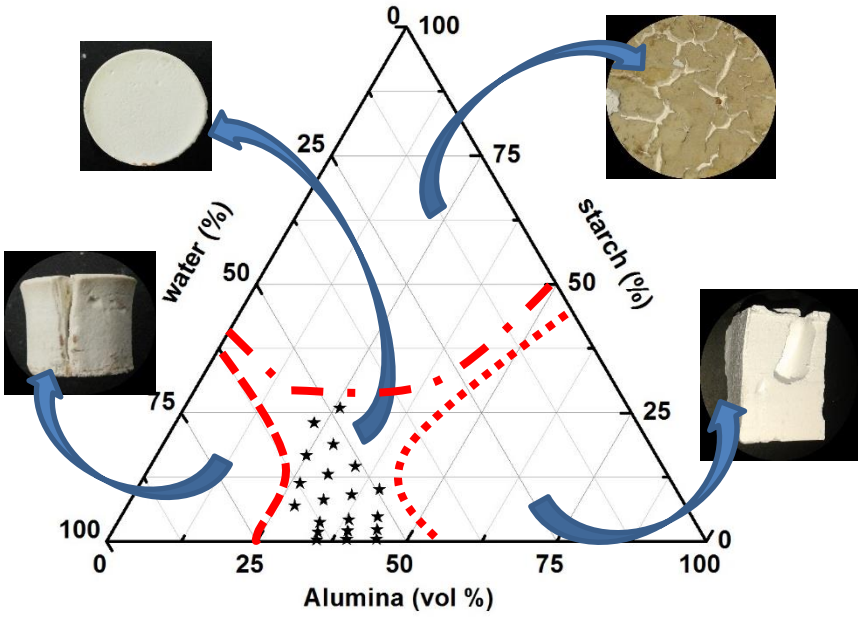


**Figure 6.9: Ternary diagram indicating slurry compositions suitable for starch consolidation casting**

In the present work the alumina loading is calculated based on alumina – water (two component system basis) and the starch, amount is calculated on the basis of alumina – starch (two component system basis). Thus, the ternary composition could be converted to two two-component basis. Figure 6.9 showed that the alumina loading of the slurry should be in the range of 30-45 vol%, and the starch content of the slurry should be in the range of 1-50 vol% to have the desired viscosity of the slurry.

Any compositions outside this range either formed cracks in the sample due to excessive drying shrinkage or it formed pinholes or blow holes due to very poor flowability (Fig 6.10). The calculation of batches based on two components and three components system and the measured viscosity of the slurry is shown in Table – VI.IV

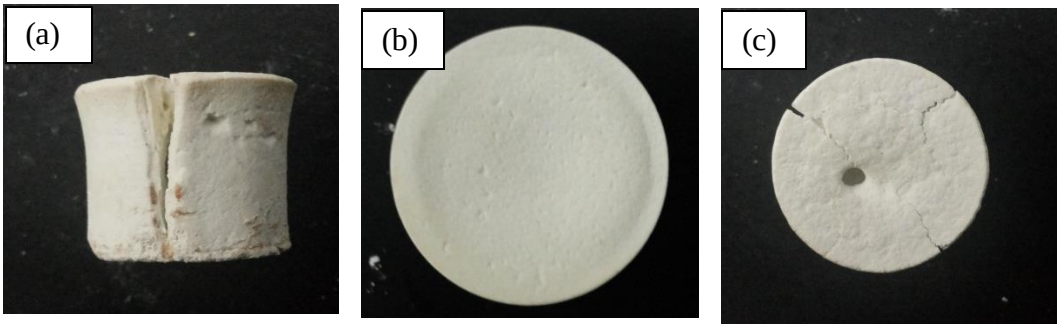


**Figure 6.10: Appearance of the samples (a) low viscosity range, (b) in the viscosity range and (c) high viscosity range.**

### 6.3.5. Green Properties

Green properties of the samples namely drying shrinkage, green porosity and strength of the starch consolidated samples as a function of alumina loading and starch content of the slurry are discussed in the following sections.

#### *6.3.5.1.Green Defects*

In the green cast body made by SCC method, the segregation of coarse particles during settling could not be clearly observed. However, the dried bodies had vertical cracks near the top surface Fig. 6.11(a). The presence of these cracks indirectly indicate a density gradient in the cast bodies which is explained below:

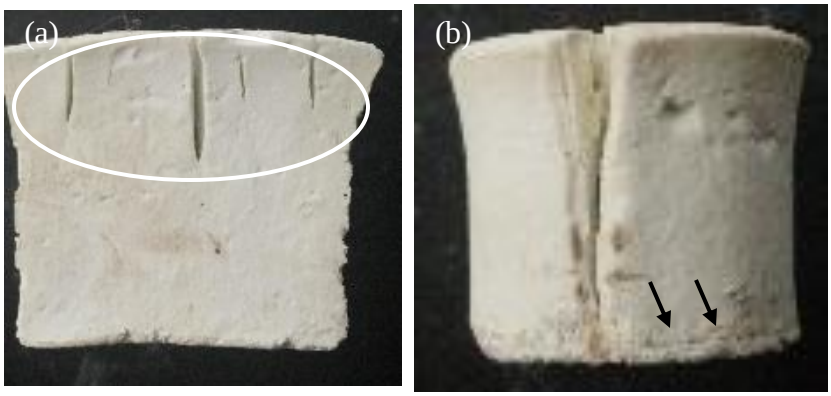


**Figure 6.11 Green defects observed in SCC technique. a) Vertical cracks near the top surface (encircled area); b) circumferential crack (arrow marked).**

During the setting of the cast, if the partial setting of the coarse particles has taken place, it will result in a better and higher particle packing at the bottom. Thus, the bottom part of the cast will have a lower shrinkage as compared to the top part. The top part being more porous will try to

shrink more during drying. The shrinkage of the top layer will be constrained by the rigid and less porous bottom part. This factor will lead to a tensile stress development at the top and cracking (encircled area). In some other sample, a circumferential crack has also been observed (Fig 6.11(b)) which has almost separated as a separate layer (arrow marked). This defect is also due to differential drying effect due to preferential settling of the coarse particles during drying.

### *6.3.5.2.Volume Shrinkage*

Starch consolidation is based on the consolidation of the ceramic slurry through gelation followed by water uptake and hydration of the starch used in the slurry. The 'as cast' slurry consists of alumina, starch, and water. It could be seen from the Table – VI.IV that alumina content in the slurry (calculated on three component basis) increases with increase in alumina loading (two component basis) whereas, the water content (calculated on three component basis) decreases. During consolidation, starch takes up some amount of water and undergoes swelling (volume expansion). This increase in the volume of the starch is equal to the volume of the water taken up by the starch during consolidation. The rest amount of water (free water) is utilized in two ways. A part of it fills up the interstitial void and the other part of water is present as a water film around the particles (alumina and swelled starch together).

The consolidated body undergoes shrinkage on drying, and this shrinkage is equal to the volume of the water film formed around the particles. The water present in the interstitial void does not have any effect on the shrinkage. The volume expansion during the consolidation of (corn) starch produces a volume stress in the matrix of cast body, which helps in rearrangement (packing) of the alumina particles. The volume stress increases with the starch content of the slurry (two component basis), and the matrix of the body containing a high amount of starch is likely to have more packing density.

The volume shrinkage of the green starch consolidated alumina samples is shown in Fig 6.12. Fig. 6.12 (a) represents the volume shrinkage of the cast as a function of alumina loading while starch content in the slurry was 20 vol%. Fig. 6.12 (b) represents the volume shrinkage of the cast as a function of starch content in the slurry while alumina loading of the slurry was 35 vol%. The volume shrinkage has been determined by measuring the volumetric changes during casting and drying of the cast.

**Table VI.IV: Composition of alumina slurry (based on two and there component system) along with its viscosity.**

| S. No | Two component system | | | | Three component system (Alumina – starch- water system) (vol%) | | | Viscosity (Pa.s) |
|---|---|---|---|---|---|---|---|---|
| | Alumina Loading (vol%) | | Starch Content (vol%) | | | | | |
| | *Alumina* | *Water* | *Alumina* | *Starch* | *Alumina* | *Starch* | *Water* | |
| 1 | 30 | 70 | 80 | 20 | 27.911 | 6.962 | 65.126 | 0.0508 |
| 2 | | | 70 | 30 | 26.590 | 11.344 | 62.064 | 0.0573 |
| 3 | | | 60 | 40 | 25.005 | 16.663 | 58.331 | 0.0683 |
| 4 | | | 50 | 50 | 23.069 | 23.069 | 53.861 | 0.242 |
| 5 | 35 | 65 | 99 | 1 | 34.873 | 0.340 | 64.785 | 0.0447 |
| 6 | | | 95 | 5 | 34.366 | 1.800 | 63.832 | 0.0491 |
| 7 | | | 90 | 10 | 33.693 | 3.721 | 62.585 | 0.106 |
| 8 | | | 80 | 20 | 32.186 | 8.041 | 59.771 | 0.139 |
| 9 | | | 70 | 30 | 30.426 | 13.042 | 56.531 | 0.160 |
| 10 | | | 60 | 40 | 28.385 | 18.903 | 52.710 | 0.234 |
| 11 | | | 50 | 50 | 25.925 | 25.925 | 48.149 | 1.19 |
| 12 | 40 | 60 | 99 | 1 | 39.847 | 0.380 | 59.771 | 0.127 |
| 13 | | | 95 | 5 | 39.175 | 2.040 | 58.793 | 0.155 |
| 14 | | | 90 | 10 | 38.295 | 4.241 | 57.462 | 0.163 |
| 15 | | | 80 | 20 | 36.367 | 9.081 | 54.550 | 0.192 |
| 16 | | | 70 | 30 | 34.146 | 14.622 | 51.230 | 1.15 |
| 17 | 45 | 55 | 99 | 1 | 44.797 | 0.440 | 54.761 | 0.301 |
| 18 | | | 95 | 5 | 43.968 | 2.300 | 53.730 | 0.348 |
| 19 | | | 90 | 10 | 42.848 | 4.760 | 52.390 | 0.825 |
| 20 | | | 80 | 20 | 40.456 | 10.104 | 49.439 | 1.980 |

Alumina loading and starch content of the slurry was found to play a vital role on the shrinkage. It could be observed from Fig 6.12[(a) and (b)] that the green volume shrinkage decreases with the increase in the alumina loading as well as the corn starch content of the slurry. The water

content and more preciously the free water content of the slurry decreases with the increase in alumina loading of the slurry (Table – VI.IV).

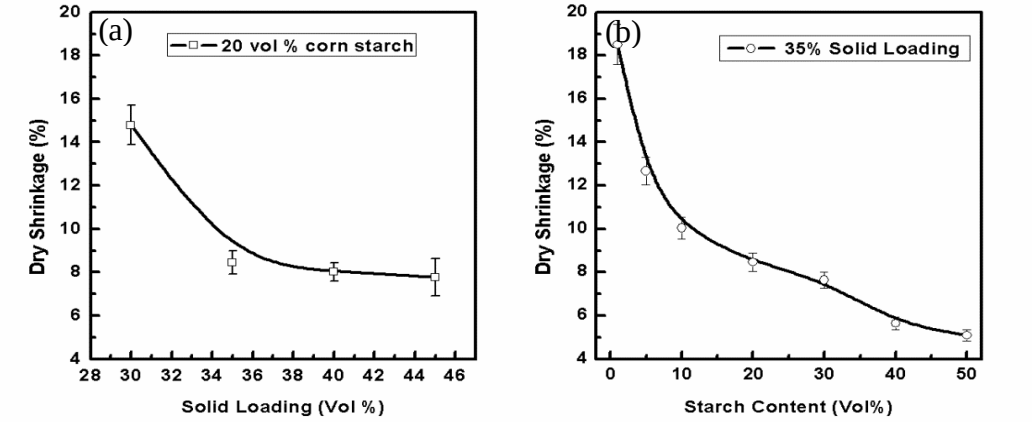


**Figure 6.12 Green shrinkage of the samples as a function of (a) solid loading and (b) starch content.**

The decrease in free water content and hence the decrease in water film thickness around the particles is attributed to the decrease in volume shrinkage of the consolidated samples. The water content and more preciously the free water content of the slurry decreases with the increase in the starch content of the slurry (Table – VI.IV). Moreover, the volume stress generated from the expansion of starch on swelling increases with the increase in the starch content of the slurry leading to better packing in the consolidated ceramics. These two facts results in low shrinkage value with an increase in starch (corn) content in the slurry.

### *6.3.5.3.Green Porosity*

The green porosity of the starch (corn) consolidated alumina samples are shown in Fig 6.13. Fig. 6.13 (a) represents the porosity as a function of alumina loading in the slurry while starch content in the slurry was 20 vol%. 6.13 (b) represents the same as a function of starch content in the slurry while alumina loading of the slurry was 35 vol%. It could be observed from Fig 6.13[(a) and (b)] that the green porosity decreases with the increase in alumina loading as well as starch (corn) content in the slurry. This is attributed to the decrease in free water content in the slurry with an increase in total solid loading (corn starch and alumina counted together) as explained earlier. Moreover, with an increase in starch content in the slurry more compactness of $Al_2O_3$ powder due to the compressive force arising from the swelling of corn starch leads to increase in packing density. As a result porosity of the sample decreases.

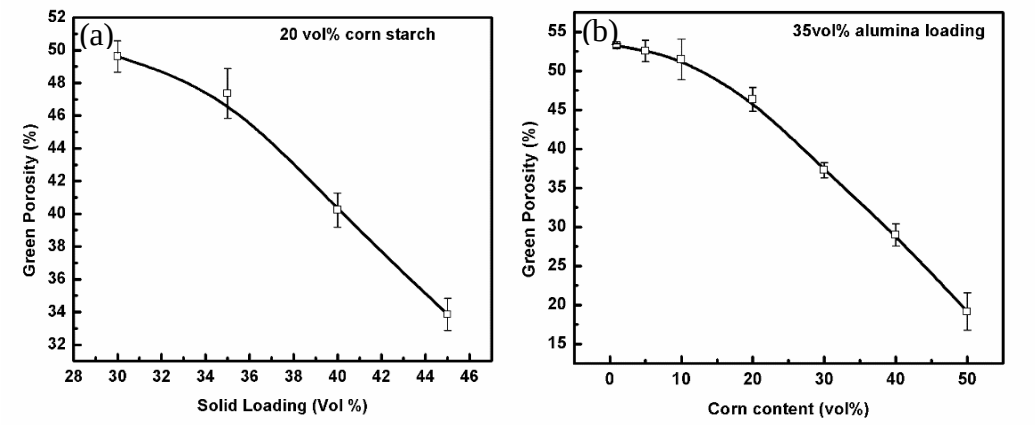


**Figure 6.13 Green porosity of the samples as a function of (a) solid loading and (b) starch content.**

### *6.3.5.4.Green Strength*

The green strength of starch consolidated alumina samples as a function of alumina loading and corn content in the slurry is presented in the Fig 6.14.

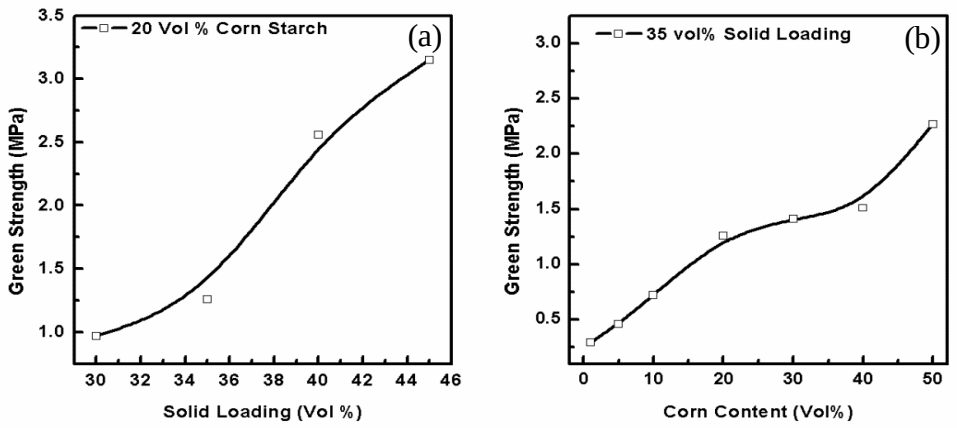


**Figure 6.14 Green strength of the samples as a function of (a) solid loading and (b) starch content.**

Fig. 6.14 (a) represents the green strength as a function of alumina loading in the slurry while starch content in the slurry was 20 vol%. Fig 6.14 (b) represents the same as a function of starch content while alumina loading of the slurry was 35 vol%. It could be observed from Fig 6.14[(a) and (b)] that the green strength increases with the increase in the alumina loading as well as with the corn starch addition. The increase in the alumina loading or the starch content in the slurry

was found to decrease the porosity of the consolidated green body. Thus, the increase in the strength for both the cases could be attributed to the decrease in porosity of the green body.

### 6.3.6. Sintered Properties

Dried green sample microstructure would consist of alumina, swelled starch and intergranular pores (packing porosity). When the dried green samples are fired at high temperature, the swelled corn burn out in the temperature zone 600-650$^{o}$C (Fig. 6.3) leading to an increase in the porosity of the sample. Thus, in the sample fired at low temperature (typically 1000$^{o}$C), the body consisted of alumina, the packing porosity and the pore formed by the pore former (pore former porosity). The volume of pore former porosity will be equal to the volume of swelled starch present in the body.

The swelled starch volume could be calculated from the volume of starch and the percentage swelling of the starch (corn) on hydration. Study of particle morphology of starch suggested a distributed particles size. Thus, the pore former porosity should have a similar distribution as that of starch. The packing pores and the pores formed by a fraction of starch are of smaller size. These small pores will collapse easily as the densification proceeds during sintering as compared to the large pores created by the pore former [16].

#### *6.3.6.1.Volume Shrinkage*

The volume shrinkage of the porous alumina samples as a function of sintering temperature, alumina solid loading and corn starch content in the slurry is shown in Fig 6.15. It could also be observed from the Fig 6.15(a) that the volume shrinkage decreased with solid $Al_2O_3$ loading when the samples were sintered at a particular temperature. Similar results were obtained for all the temperature studied in the present study. There was an appreciable change in volume shrinkage (5-7%) as a function of alumina loading when the samples were sintered at low temperature (1300-1400$^{o}$C). However, it was small (2-3%) when the samples were sintered at high temperature (1500-1600$^{o}$C). The porosity of the dried cast samples (Section 6.3.5.2) was found to decrease with alumina loading. Thus, the sample prepared with high alumina solid loading slurry were likely to have small packing porosity as compared to that prepared with low solid loading. This packing porosity is likely to disappear at low sintering and is associated with shrinkage. Thus, the samples prepared with low alumina loading slurry showed high shrinkage when sintered at low temperature. The rapid increase in volume shrinkage observed in the

temperature range 1400-1500°C is attributed to the enhanced sintering of the sample at this temperature.

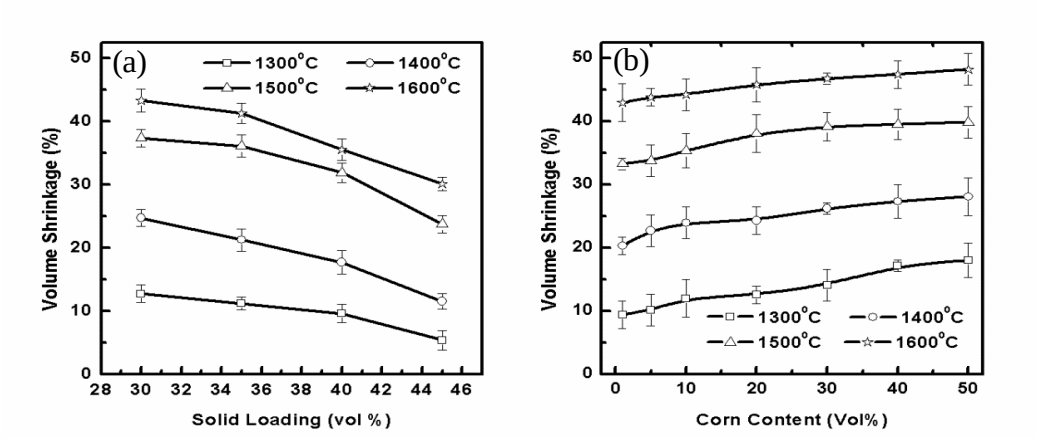


**Figure 6.15 Sintered shrinkage of the samples as a function of (a) solid loading and (b) starch content as well as sintering temperature.**

It can be seen from Fig 6.15(b) that the volume shrinkage of the sample increases with corn content in the slurry. Firing shrinkage is associated with the disappearance of pores on densification. Small size pores disappear easily during sintering as compared to that having a large size. The pore former used in the present study has distributed particle size (Fig 6.2) which produces distributed pores on its removal during the firing process. The amount of pores generated by the pore former increases with the increase in starch content in the slurry. Thus, the pore former porosity increases in the samples prepared with high starch content in the slurry. A major portion of the packing porosity and a fraction of pore former porosity are likely to disappear during densification. The second part increases with increase in starch content in the slurry. Thus, the samples prepared with high starch content showed high shrinkage. It can be seen that the volume shrinkage increases with the increase in sintering temperature irrespective of the amount of the corn starch added. This is correlated with the densification of alumina with temperature.

*6.3.6.2.**Apparent Porosity***

The influence of the alumina loading, corn starch content and sintering temperature on the apparent porosity of the starch consolidated alumina samples is presented in the Fig. 6.16. The porosity decreases with the increase in the $Al_2O_3$ loading as well as the sintering temperature [Fig 6.16 (a)].The green porosity (or packing porosity) decreases with increase in the alumina loading (Fig 6.13). The decrease in green porosity with an increase in alumina loading indicated

improved packing of alumina in the consolidated body. Thus, the smaller size pores (interparticle porosity) are expected to be small in a sample prepared with high alumina loaded slurry. These samples will show less porosity on sintering also. Thus, the apparent porosity of the samples decreases with increase in alumina loading in the slurry.

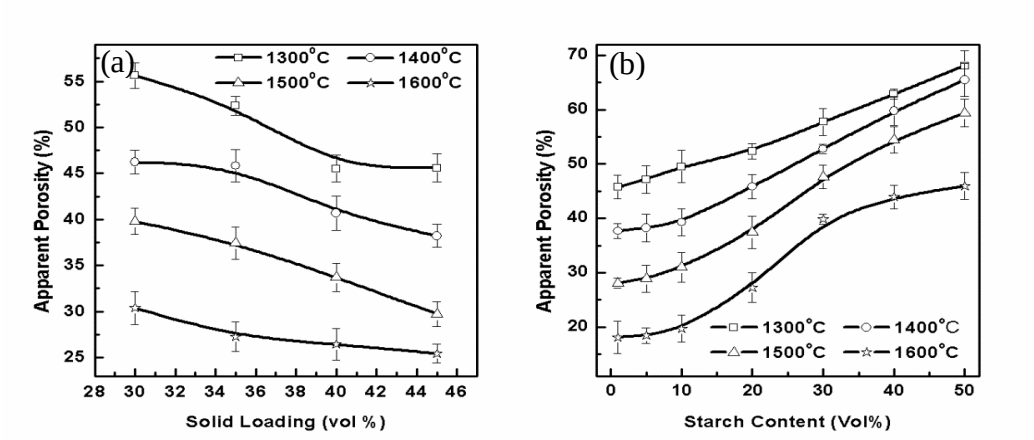


**Figure 6.16 Sintered porosity of the samples as a function of (a) solid loading and (b) starch content as well as sintering temperature.**

It could also be observed from the Fig 6.16(b) that with the increase in the corn starch content the apparent porosity increases. The combustion of corn starch in the temperature 600-650°C (Fig. 6.3) creates pores (pore former porosity) in the alumina matrix. The packing porosity decreases with the increase in the starch content (Fig 6.13). Pore former porosity should have distributed size as that of the starch used in the study. A fraction of the pore former porosity and the packing pores disappears with the progress in the densification due their small size. However, with the increase in the starch content the porosity increases in spite of the fraction of pores getting disappeared during densification. It could be seen that apparent porosity decreases with the increase in the sintering temperature and is correlated with the densification of the samples at high temperature.

### *6.3.6.3.Relative Density*

Figure 6.17 presents temperature dependence of the relative density of the porous alumina sample prepared by starch consolidation technique as a function of alumina loading and starch content in the slurry. It could be observed from Fig 6.17(a) that the relative density increases with the increase in the alumina loading. It could be seen from Fig. 6.13 that the green porosity of the sample decreases with increase in solid loading of the slurry. Thus, the samples prepared

with high solid loading slurry would have more green density. Better the green density of the sample better the sintered density. Thus, the relative density of the sample increases with alumina loading of the slurry

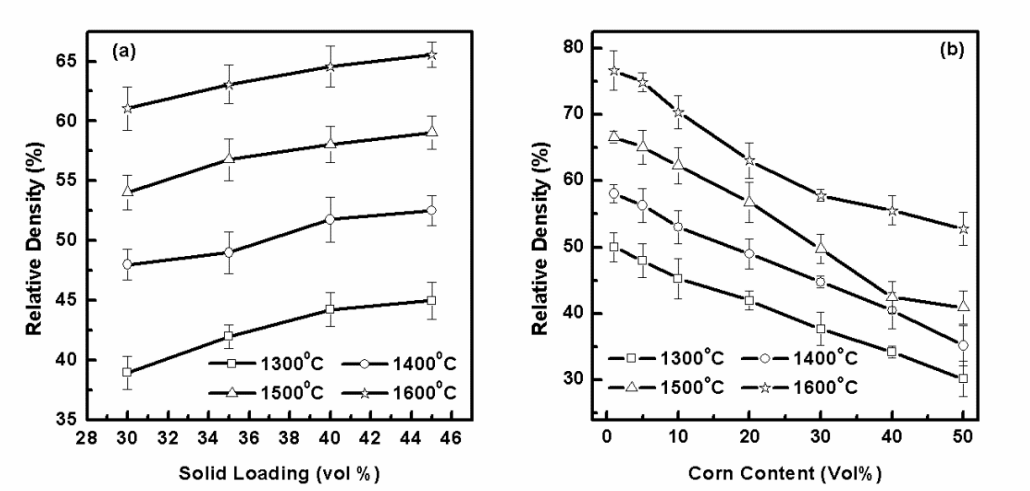


**Figure 6.17 : Sintered density of the samples as a function of (a) solid loading and (b) starch content as well as sintering temperature**

Figure 6.17(b) represents that relative density of the sample decreases with the increase in the corn starch content in the slurry. The starch granules present in the samples burn off leaving the pores in the samples. Thus, the density of the sample decreases with increase in starch amount in the slurry. Relative density as a function of sintering temperature was found to increase in both the cases. This is attributed due to the increase in densification with the increase in the sintering temperature.

### *6.3.6.4.Cold Crushing Strength*

Cold crushing strength (CCS) of porous alumina ceramics prepared by starch consolidated technique has been shown in Fig. 6.17 as a function of sintering temperature, alumina loading and corn starch content in the slurry. Figure 6.18(a) shows that the CCS increases with the increase in the alumina loading. The increase in CCS value with an increase in alumina loading of the slurry could be correlated to the increase in the density as explained earlier. CCS of the sample was found to decrease with increase in corn starch content in the slurry (Fig 6.18(b)). Corn starch produces pore former porosity in the samples. Thus, pore former porosity in the samples increases with increase in corn starch content of the slurry. This increase in pore former porosity with an increase in starch content is correlated with the decrease CCS value observed in

the sample. CCS of the sample was found to increase with an increase in sintering temperature in both the cases. Porous alumina sample sintered at 1600°C showed highest strength value (81.77 MPa) which is almost four times that observed for the sample sintered at 1300°C which has a compressive strength of 19.27 MPa. It has been discussed earlier that the porosity of the samples decreases with increase in sintering temperature and is attributed to densification of the samples at high temperature. Thus, the increase in CCS value of the samples with an increase in sintering temperature is correlated with the decrease in the porosity of the samples with an increase in sintering temperature.

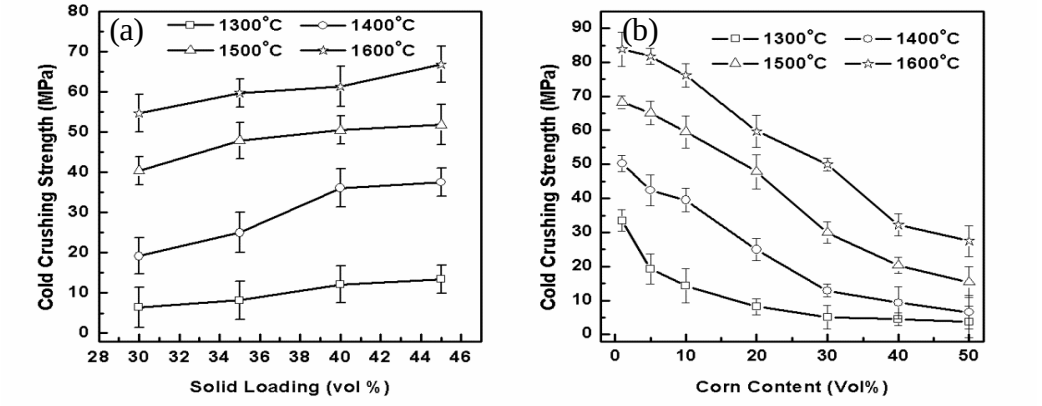


**Figure 6.18 Cold Crushing Strength of the samples as a function of (a) solid loading and (b) starch content sintered at different sintering temperatures**

### *6.5.6.5. Microstructure*

The microstructure of the porous alumina samples fabricated through starch consolidation technique has been shown in the Fig 6.19. Fig 6.19 [(a) and (b)] represents the microstructure of the 1600°C sintered sample containing 30 vol % and 45 vol % alumina loading respectively with 20 vol% corn starch. The presence of large interconnected pores in the matrix containing small pores could be observed from both micrographs. The large pores are formed due to burning off the starch and are the pore former porosity in the samples. The small pores observed in the matrix are interparticle porosity (packing porosity). It could also be observed that the population of interparticle porosity decreases with increase in alumina loading and thus supports the earlier observations.

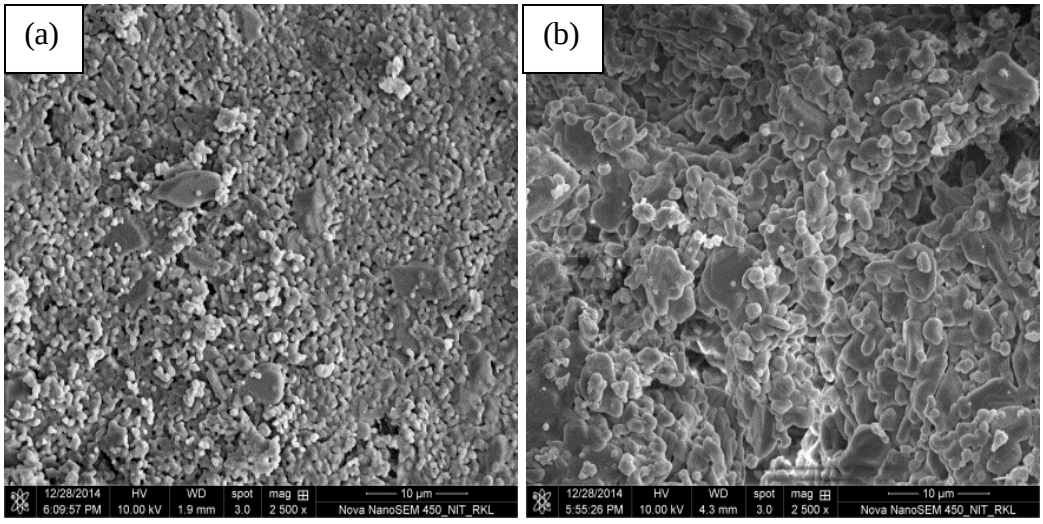


**Figure 6.19 SEM micrograph of the samples prepared with (a) 30 vol% and (b) 45 vol% alumina loaded slurry containing 20 vol% starch sintered at 1600°C.**

The SEM micrographs of the samples prepared with a 35% alumina loaded slurry containing 20 vol% and 40 vol% corn starch has been shown in Fig. 6.20 [(a) and (b)] respectively.

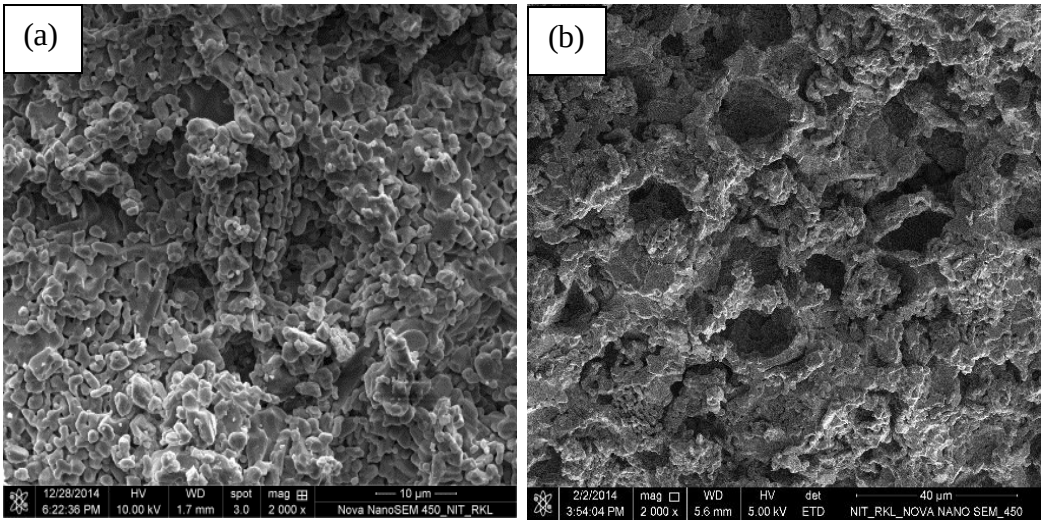


**Figure 6.20 SEM micrograph of the samples prepared with 35 vol% alumina loaded slurry containing (a) 20 vol% and (b) 40 vol% starch sintered at 1600°C.**

The samples have been sintered at 1600°C. It could be observed that with the increase in the corn starch content the large pores (pore former porosity) in the samples increases, whereas, the small sized intergranular porosity (packing porosity) decreases.

It could also be observed that with the increase in the pore former, the interconnections between the pore former (corn starch) pores increases. The increase in pore former porosity is attributed to the increase in starch content in the slurry. The decrease in interparticle porosity is related to the combined effect of the decrease in water content of the slurry as well as an increase in compressive stress in the slurry due to swelling of the starch

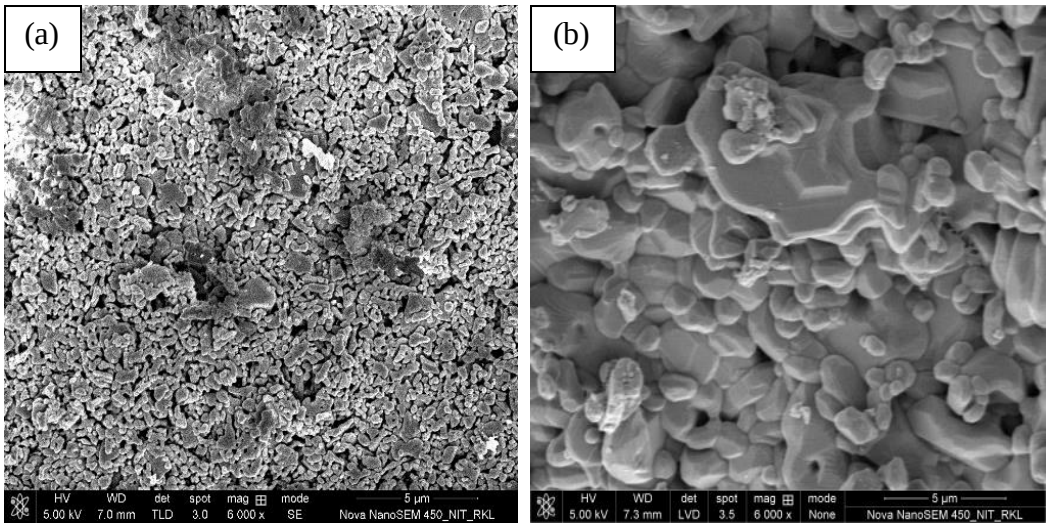


**Figure 6.21 SEM micrograph of the samples prepared with 35 vol% alumina loaded slurry containing 1 vol% starch sintered at (a) 1300°C and (b) 1600°C.**

The microstructures of the samples prepared with 35 vol% alumina loaded slurry containing 1vol% starch sintered at 1300°C, and 1600°C has been shown in Fig. 6.21[(a) and (b)] respectively. Two distinct features could be revealled from the micrographs. First one is the interparticle porosity was found to be more when the samples were sintered at low temperature (1300°C). Second is the grain size of the samples was found to be more in the samples sintered at high temperature (1600°C). These features could be correlated with the densification and grain growth of the samples associated with the temperature. The extent of densification and grain growth is expected to be low when the samples are sintered at low temperature. Thus, the samples sintered at 1300°C showed more interparticle porosity and small grain size.

### 6.3.7. Validation of Theoretical Model

The porosity of the porous sample depends on several parameters like percent swelling of starch, starch and water content in the slurry. Theoretical calculation cited in Chapter 5 shows that if green and firing shrinkage of starch consolidated body is known the porosity of the samples can be predicted.

The green porosity of the starch consolidated body is due to the removal of water present in the intergranular space of the particles. These are mostly open pores. Thus, the apparent porosity of the green samples are close to the total porosity. The porosity of the starch consolidated samples as a function of alumina loading and starch content has been shown in Fig. 6.22.

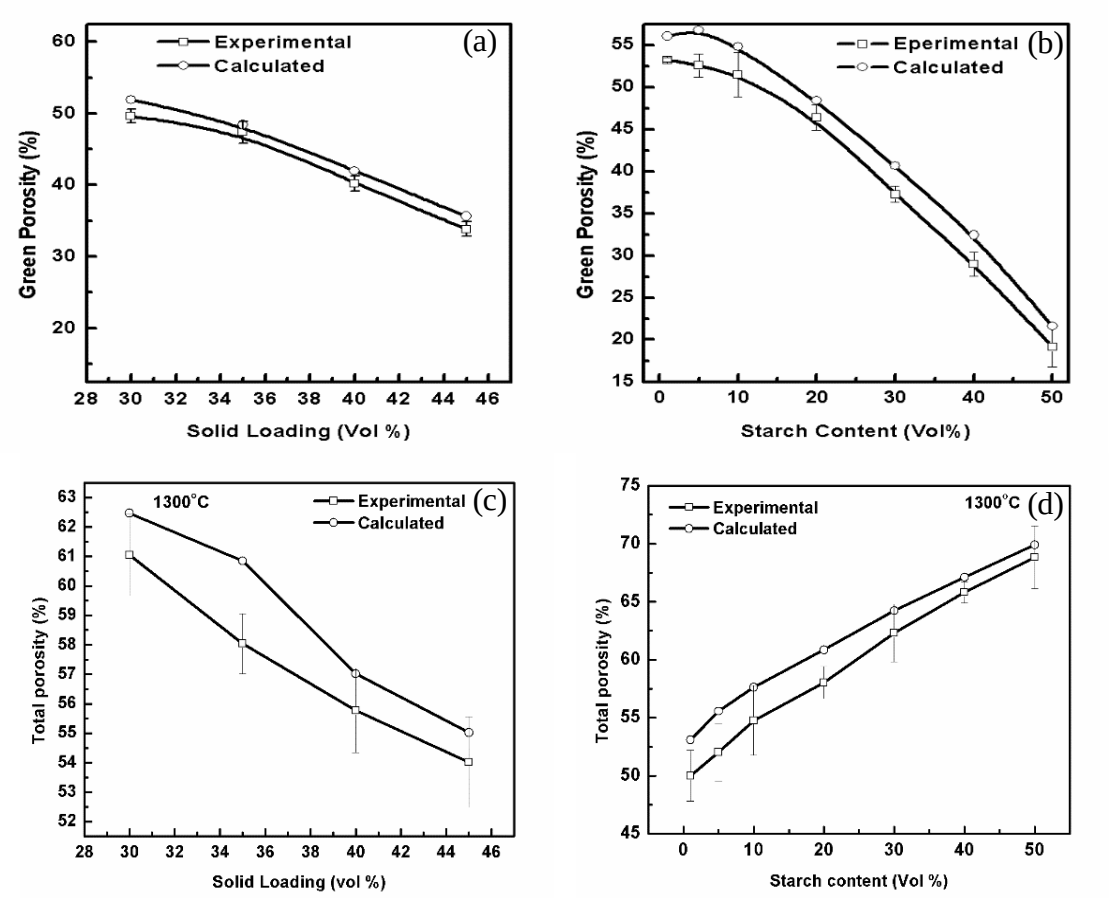


**Figure 6.22 Green and sintered porosities of the samples showing the validation of the theoretical model.**

Fig 6.22 [(a) and (b)] represents measured green porosity of the samples as a function of alumina loading and starch content in the slurry respectively. The porosity of the sample calculated using the equation 5.12. Has also been incorporated into the figure. It could be seen that the theoretical green porosity calculated using equation 5.12 matches well with the measured one. Fig 6.22 [(c) and (d)] represents measured sintered porosity of the samples sintered at 1300°C as a function of alumina loading and starch content in the slurry respectively. The porosity of the sample calculated using the equation 5.14 has also been incorporated into the figure. It could be seen that

the theoretical porosity calculated using equation 5.14 matches well with the measured one with a small deviation. The deviation in the values is due to the assumptions made in the model

### 6.3.8. Effect of Type of Starch

The effect of type of starch on sintered volume shrinkage, apparent porosity, relative density and cold crushing strength (CCS) of porous alumina ceramics as a function of sintering temperature prepared by SCC technique has been shown in Fig 6.23. All the samples have been prepared with 35 vol% alumina loaded slurry containing 30 vol% starch. It could be seen from the Fig 6.23(a) that the sintered volume shrinkage is almost similar irrespective of the type of starch.

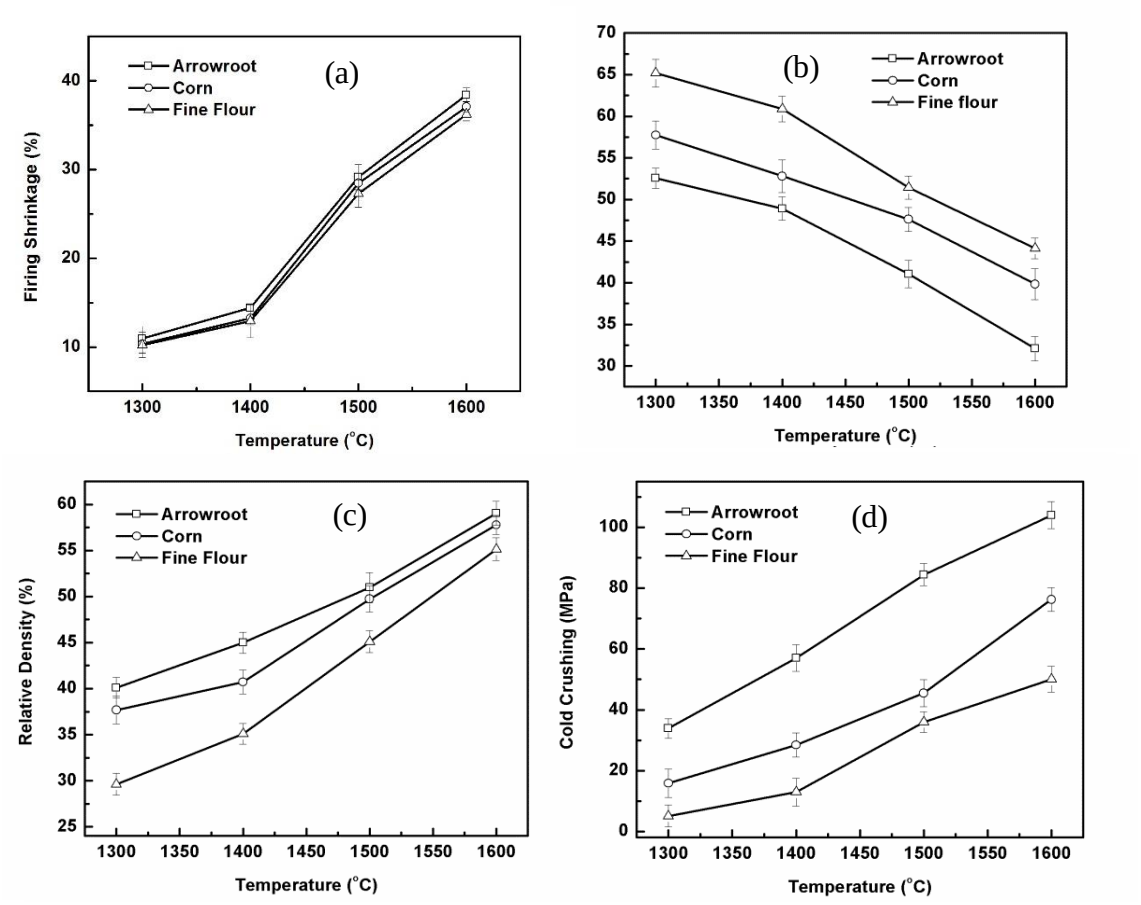


**Figure 6.23 Influence of sintering temperature on (a) volume shrinkage, (b) apparent porosity, (c) relative density and (d) cold crushing strength of the samples prepared with different type of starch.**

The volume shrinkage increases with increase in sintering temperature and is correlated to the densification of the sample with an increase in temperature. The shrinkage is mainly due to the disappearance of smaller size pores (interparticle pores and a fraction of pores formed from the

small size fraction of the pore former used) present in the body. It could also be observed that variation in the volume shrinkage is 5% between 1300-1400°C, 15 % between 1400-1500°C and 10% between 1500-1600°C irrespective of the type of starch. This rapid change between 1400-1500°C is due to the progress in the densification of the samples. Figure 6.23(b) presents the influence of the type of starch on the apparent porosity of the alumina samples. It could be observed that irrespective of the sintering temperature, the porosity of the samples prepared with fine flour is higher as compared to that prepared with corn and arrowroot. Samples prepared with arrowroot starch have the smallest porosity value while those prepared with corn starch showed an intermediate value. Swelling behavior study indicated that fine flour undergoes the highest swelling among the three starches, while arrowroot has the smallest swelling and corn has an intermediate swelling. Thus, the samples prepared with fine flour showed the highest porosity. The porosity of the samples prepared with all the starches decreases with increase in sintering temperature and is related to the densification of the sample.

The relative density of the samples as a function of the starch type and sintering temperature has been shown in the 6.23(c). It showed the exactly the opposite trend as that of porosity and were quite obvious. This behavior could be explained in terms of the swelling of the starch and its consequences on the packing behavior during the consolidation process. The cold crushing strength of the samples as a function of the starch type and sintering temperature has been shown in Fig 6.23(d). The CCS of the samples is 40.11MPa, 37.68MPa, 29.62MPa at 1300oC and 59.04MPa, 57.78MPa, 55.14MPa at 1600oC for arrowroot, corn starch, and fine flour respectively. Samples prepared with arrowroot showed the highest strength while that prepared with fine flour showed the lowest strength value when sintered at the same temperature. The samples prepared with corn starch showed an intermediate value. The observed CCS value in the samples could be correlated with the porosity of the samples

#### *6.3.8.1.Microstructure*

The microstructure of porous samples fabricated using a different type of starch has been shown in the Fig. 6.24. The samples were sintered at 1600°C. Figure 6.24(a) shows the distribution of pore former porosity in a sample prepared with 35 vol% of alumina loaded slurry containing 30 vol % arrowroot starches. It could be observed that the pores are irregular in nature with a pore

size ranging from 11-32µm same as the granular size of the arrowroot starch. Hence, the large pores were the pore former pores.

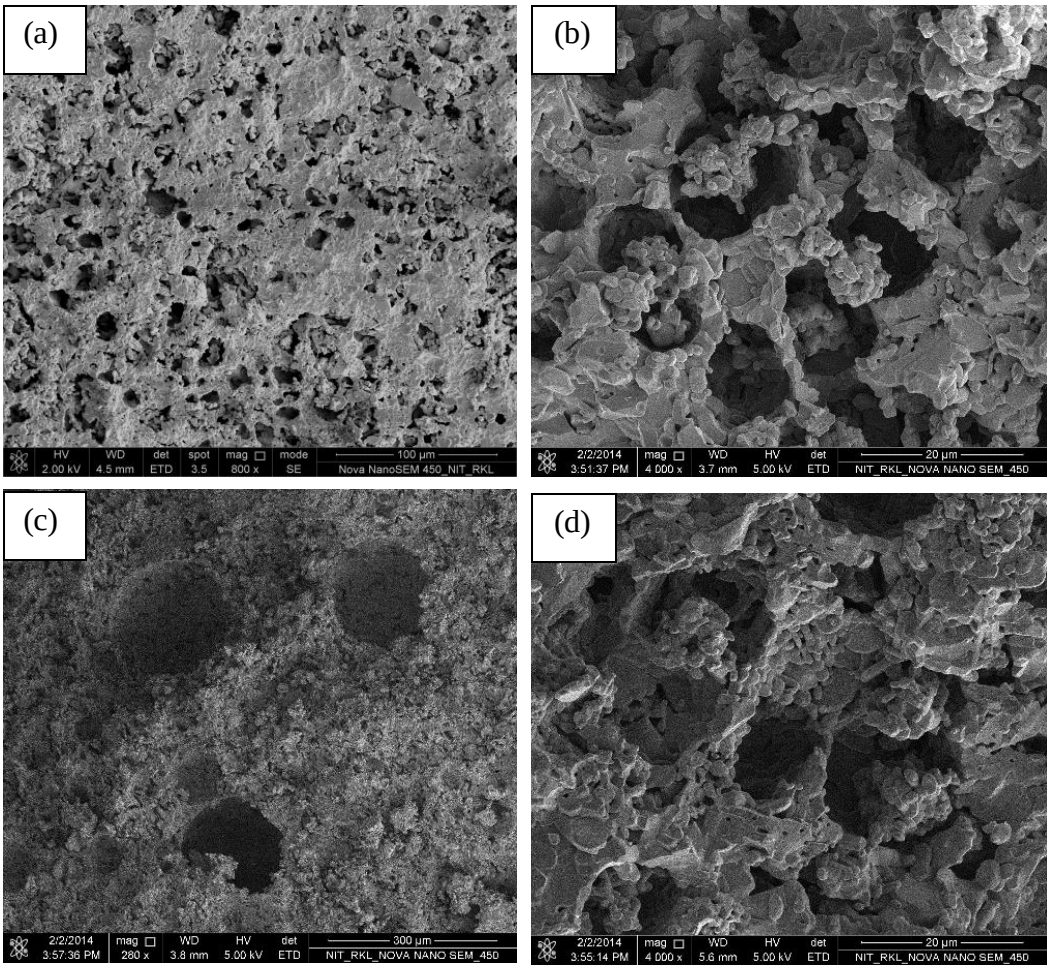


**Figure 6.24 SEM Micrographs porous alumina ceramics prepared with 35 vol % alumina loaded slurry containing 30 vol % starch (a) arrowroot, (b) corn, (c) arrowroot, and (d) fine flour.**

Figure 6.24[(b), (c) and (d)] represent the pores created by the pore formers corn starch, arrowroot and fine flour respectively. Corn pores [Fig. 6.24(b)] showed both small and large size pores. The pore size distribution is in the range of 6-18µm. It could be observed that the particles are spherical in shape. Arrowroot pores [Fig. 6.24(c)] showed irregular shape with distributed pore size in the range of 11-32µm. Fine flour pores [Fig. 6.24(d)] are spherical in shape and have the size distribution in the range of 3-13µm.

### 6.3.9. Effect of Titania Addition

Titania has been used as a sintering additive to increase the strength of the porous alumina samples. The presence of $TiO_2$ progresses the densification of the sample. Lowering the sintering temperature without compromising the porosity and the strength of the sample could be possible by the addition of $TiO_2$.

The effect of titania ($TiO_2$) on the properties of the porous alumina samples is represented in the Fig 6.25. The samples are prepared with alumina loading of 45 vol% with a corn content of 1 vol% related to the alumina powder. These are sintered at 1500°C to optimize the $TiO_2$ amount. Apparent porosity as a function of $TiO_2$ addition is shown in the Fig 6.25(a). It could be observed from the Fig 6.25 that $TiO_2$ addition reduces the porosity of the samples. It could also be observed that a small amount of $TiO_2$ addition (up to 3 wt%) is more effective in lowering the porosity of the sample. The total porosity of the samples decreased to 15% with the addition of 1 wt% $TiO_2$, which is twice the porosity that observed in the samples prepared without $TiO_2$ additive. Fig 6.25(b) shows the CCS of the samples as a function of $TiO_2$. The CCS followed an inverse relation with the porosity. The sintering and the grain growth of alumina were influenced by the addition of the $TiO_2$. $TiO_2$ has a substantial solubility in $Al_2O_3$ matrix. The solubility limit of $TiO_2$ in $Al_2O_3$ is limited to 0.35mol% (70-71). Substitution beyond this limit leads to precipitation of the second phase of $Al_2TiO_5$ (71-73). The $TiO_2$ addition was only 3wt% in the present study that is well below the solubility limit. Substitution of $Al^{3+}$ sites by $Ti^{4+}$ ions within the solubility limit leads to the formation of aluminium vacancies ($V_{Al}^{'''}$). The defect formation reaction can be written as follows:

$$3TiO_2 \xrightarrow{2Al_2O_3} 3Ti_{Al}^{\bullet} + 6O_O^{\times} + V_{Al}^{'''}$$

The densification of $Al_2O_3$ ceramics was enhanced by the diffusion of the aluminium vacancies ($V_{Al}^{'''}$) [70-73].

The effect of sintering aid $TiO_2$ on the porosity and compressive strength of the porous alumina samples is shown in the Fig 6.25. It could be observed from the Fig 6.25(c) that the 20% of porosity decreases with the addition of $TiO_2$. It could also be observed that the porosity of the samples sintered at 1600°C without $TiO_2$ and the porosity of the samples sintered at 1300°C with $TiO_2$ were almost similar irrespective of the starch content in the sample

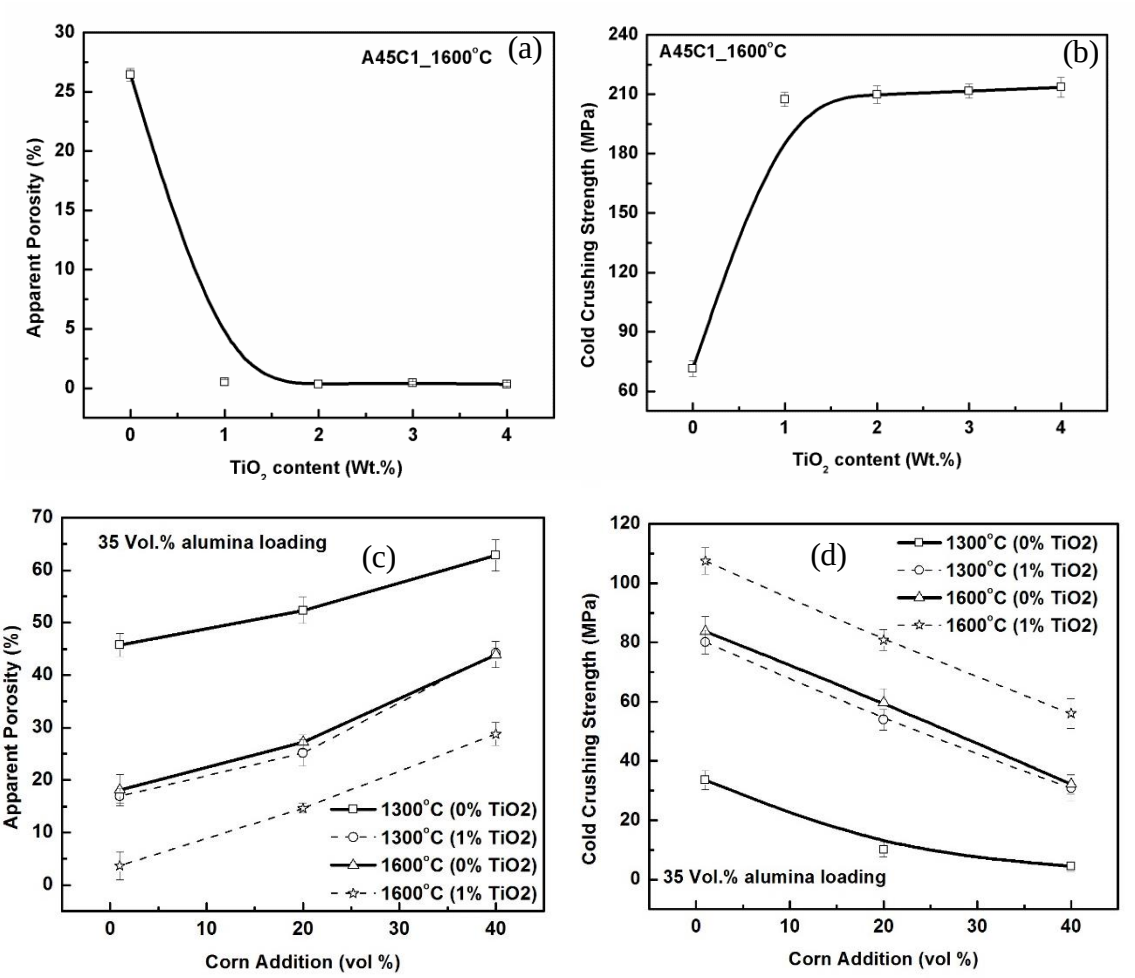


**Figure 6.25 Effect of $TiO_2$ addition on (a) apparent porosity, and (b) cold crushing strength of the samples prepared with 45 vol% alumina loading slurry containing 1 vol% corn sintered at 1600°C; (c) apparent porosity and (d) cold crushing strength of the samples**

Figure 6.25(d) shows that the cold crushing strength increases with the addition of $TiO_2$. It could be seen that the similar compressive strength is obtained for the samples sintered at 1600°C without $TiO_2$ and the porosity of the samples sintered at 1300°C with $TiO_2$. Hence from this study it could be concluded that the lowering of sintering temperature could be possible by the addition of $TiO_2$ without compromising the porosity and the strength of the porous alumina samples.

### *6.3.9.1.Microstructure*

The effect of $TiO_2$ additive on the microstructure of the porous samples prepared by starch consolidation technique has been represented in the Fig 6.26. The microstructure of the 0wt%

and 1wt% $TiO_2$ added sample prepared with a sulrry containing 35vol% of alumina loading and 1vol% of the corn starch are shown in Figure 6.26[(a) and (b)] respectively.

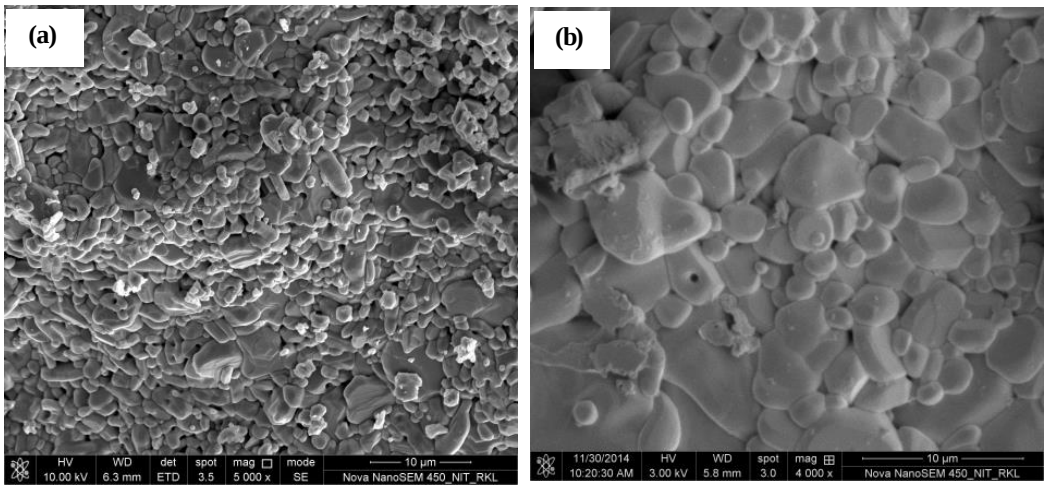


**Figure 6.26 SEM micrographs of the samples prepared with 35 vol% alumina loading slurry containing 1 vol% corn starch sintered at 1600°C (a) 0% $TiO_2$, (b) 1% $TiO_2$**

Fig 6.26[(a) and (b)] show that with the addition of the additives enhanced the grain growth leading to increasing in shrinkage and strength as well as a decrease in the porosity. This change in the properties has been attributed to the enhanced grain growth with the addition of the additives.

The microstructure of the sample prepared with 20 vol% corn starch and sintered at 1600°C and 1300°C has been shown in Fig. 6.27[(a) and (b)] respectively, where, sample sintered at 1600°C does not contain any $TiO_2$, and that sample sintered at 1300°C contains 1wt% $TiO_2$. It is worthy to note that the microstructural features namely grain size and its distribution, pore size, and its distribution were found to be quite identical in both the micrographs. These features support the observed identical physical properties of the samples sintered at 1600°C without $TiO_2$ and 1300°C with $TiO_2$. Hence, the study suggests that $TiO_2$ addition is effective to reduce the sintering temperature of porous alumina ceramics without compromising the porosity and strength. All the samples prepared hence fourth in SRT and combination technique contain 1% $TiO_2$ as a sintering additive.

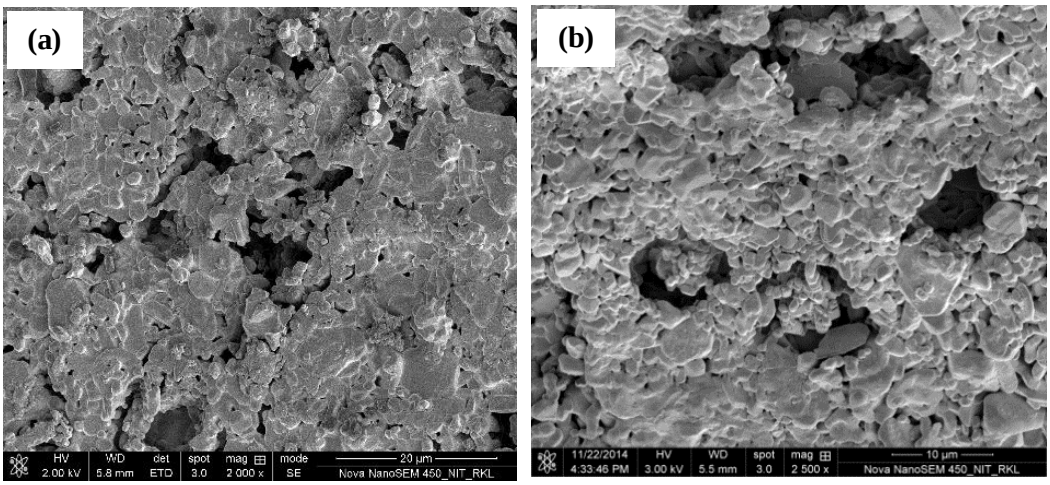


**Figure 6.27 SEM micrographs of the samples prepared with 35 vol% alumina loading slurry containing 1 vol% corn starch (a) 0% $TiO_2$ sintered at 1600oC (b) 1% $TiO_2$, sintered at 1300°C**

## 6.4. Sponge Replica Technique

The most frequently used technique, in order to obtain a highly interconnected porous structure is the sponge replica technique. The porous structure and its properties like apparent porosity and the cold crushing strength of the samples were more dominated by the particle loading, rheology of the slurry and the structure of the polymeric sponge template. Particle loading and the sintering temperature depicts the strength of the porous sample.

### 6.4.1. Rheological Behaviour of Slurry Suitable for SRT Technique

The slurry for the sponge replica technique should have the capability to coat the struts of the template (sponge) uniformly and should not drain out of the template after impregnation. The rheological behaviour of the slurry with different solid loading has been represented in the Fig 6.28(a). It could be observed that all the slurries exhibit shear thinning behaviour and the shear thinning hysteresis decreases with the decrease in the solid loading. The viscosity of the slurry decreases with a decrease in the solid loading that has been attributed to the breakdown the flocs present in the slurry by applying the shear.

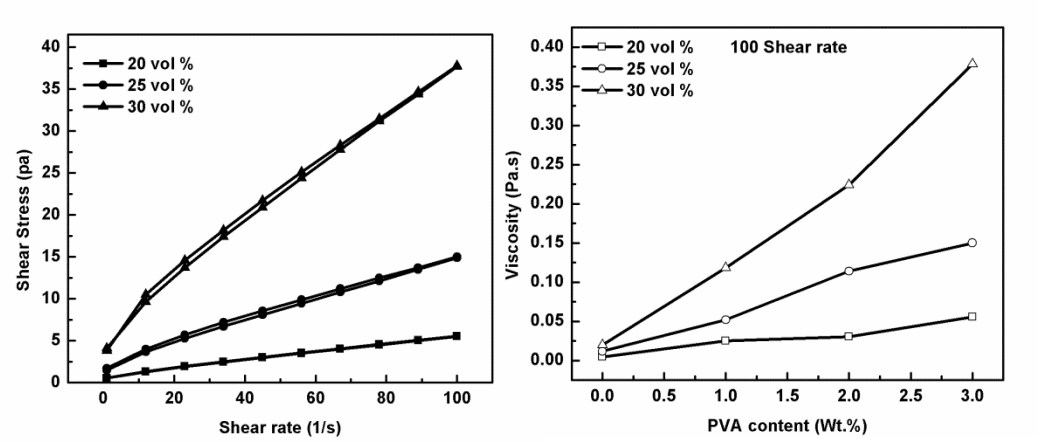


**Figure 6.28 Rheological behavior of $Al_2O_3$ slurry showing (a) shear stress-shear rate behavior (b) effect of PVA content on the viscosity of the slurry as a function of alumina loading**

### 6.4.2. Viscosity and Binder Optimization

Figure 6.28(b) shows the effect of the binder (PVA) on the viscosity of the slurry as a function of solid loading. It has been observed that the viscosity of the slurry increases with the increase in the binder content. This could be attributed to the presence of active polymer that decreases the relative motion of the ceramic particles in the slurry leading to the increase in the viscosity. It has been observed that the viscosity increases with the increase in the solid loading at a particular binder content. This could be correlated to the powder agglomeration in the slurry. At high solid loading slurry, the viscosity was found to be strongly dependent on shear rate as compared to that observed in slurry prepared with low solid loading.

### 6.4.3. Sintering Properties

#### *6.4.3.1.Volume Shrinkage*

The sintered volume shrinkage of the porous alumina samples fabricated using sponge replica technique as a function of sintering temperature as well as alumina solid loading in the slurry is shown in Fig 6.29. It could also be observed that the volume shrinkage decreased with the increase in solid $Al_2O_3$ loading of the slurry when the samples were sintered at a particular temperature. With the increase in the alumina loading from 20-35 vol %, the volume shrinkage decreased from 15-8 % when the samples were sintered at 1400°C while it decreased from 21-14% when sintered at 1600°C.

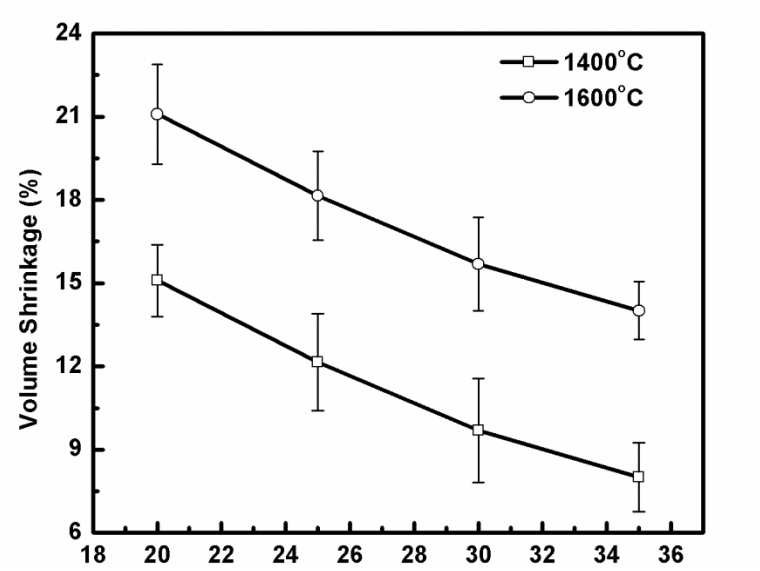


**Figure 6.29 Volume shrinkage of the sponge replica samples as a function of alumina loading and sintering temperatures.**

The water content of the slurry calculated on three component basis decreases with increase in alumina loading (two component basis). The decrease in the water content causes an increase in strut thickness and more number of filled structure formed during fabrication. Thus, a dense microstructure is likely to form when the samples are prepared with high alumina solid loading. The decrease in the volume shrinkage with the alumina loading has been attributed to the decrease in the free water in the slurry and the consequent effects of the same. It could also be observed that the volume shrinkage was more when the samples were sintered at high temperature. The increase in volume shrinkage with an increase in sintering temperature is correlated with the sintering behaviour. The high the sintering temperature the more will be densification. Moreover, in the present case the sample is prepared with $TiO_2$ as an additive that forms a liquid phase at high temperature and showed enhanced densification. Volume shrinkage always accompanies densification. Thus, the volume shrinkage increases with increase in sintering temperature.

### *6.4.3.2.Apparent Porosity*

The influence of the alumina loading of the slurry and sintering temperature on the apparent porosity of the porous alumina samples prepared by sponge replica technique is presented in the Fig 6.30. The porosity decreases with the increase in the $Al_2O_3$ loading as well as the sintering temperature. The porosity of the samples decreased from 81-72% with the increase in the alumina loading from 20-35 vol% when the samples were sintered at 1400°C.

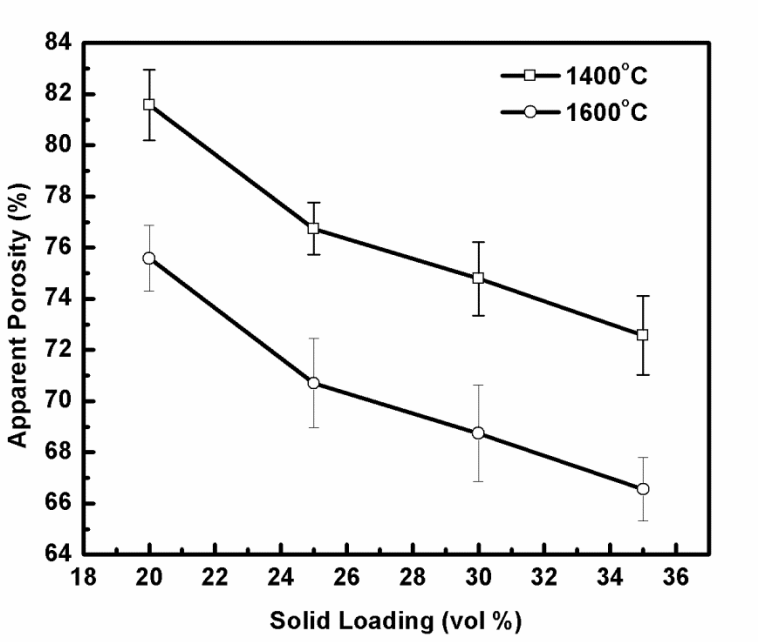


**Figure 6.30 Apparent porosity of the sponge replica samples as a function of alumina loading and sintering temperatures**

The water content of the slurry decreases with increase in alumina loading when calculated based on three components. The decrease in the water content may lead to an increase strut coating thickness and more filling of pore the sponge during the fabrication process. Thus, the samples prepared with high alumina solid loading are expected to have a dense structure as compared to that prepared with low alumina solid loading samples. The porosity decrease with the increase in the alumina loading has been attributed to the increase in the strut thickness and the pore filling of the template. The porosity of the sample was found to decrease with the increase in sintering temperature. This is quite obvious and is correlated to the enhanced densification of the sample at elevated temperature.

### *6.4.3.3.Cold Crushing Strength*

Cold crushing strength (CCS) of the samples prepared by sponge replica technique as a function of alumina loading and sintering temperature is shown in the Fig 6.31. The CCS increased from 0.65-2.46 MPa when the samples were prepared with alumina solid loading 20-35 vol %. The observed increase in CCS value with an increase in the alumina loading of the alumina slurry is correlated to the enhanced packing of the alumina particles with a decrease in the free water in the slurry. The increase in alumina loading in the slurry may also increase the strut and pore wall thickness of the sample.

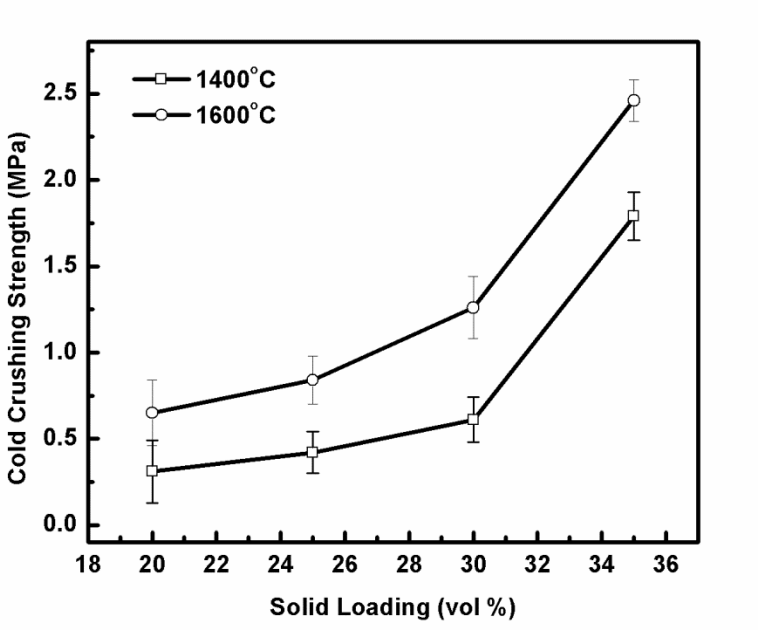


**Figure 6.31 Cold crushing strength of the sponge replica samples as a function of alumina loading and sintering temperatures.**

Thus, the increase in CCS value with an increase in alumina loading in the slurry is attributed to the decrease in porosity as well as an increase in strut and pore wall thickness. It could also be observed that the CCS value increased from 0.31-1.79MPa when the samples were sintered at 1400°C and 1600°C respectively. The density of the samples was found to increase with an increase in sintering temperature. Thus, the increase in strength with the sintering temperature may be correlated to the decrease in the porosity of the samples associated with enhanced densification at high temperature.

### *6.4.3.4.Microstructure*

The SEM micrographs showing the effect of alumina loading of the slurry and the sintering temperature on the porous alumina samples fabricated with polymeric sponge replica technique has been shown in the Fig 6.32. The samples were prepared with a slurry having alumina loading in the range 20vol% to 35vol% (two component basis) and were sintered at 1400 and 1600°C. The presence of large pores interconnected pores, typical characteristics of sponge replica technique could be observed from the micrographs. These pores forms due to burning out of polymeric sponge template and are characteristics of the sponge template used. Sponge replica technique produces positive morphology of the template used.

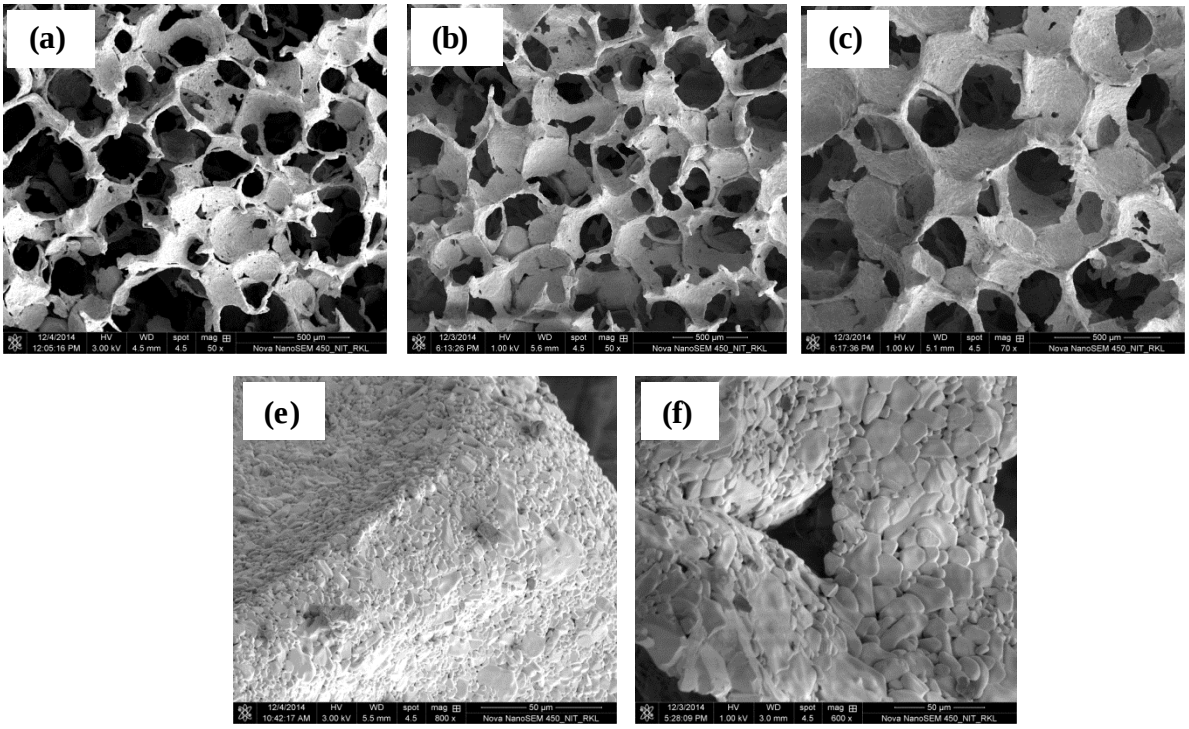


**Figure 6.32 SEM micrograph of sponge replica samples prepared with (a) 25vol%, (b) 30vol% and (c) 35vol% alumina loading slurry sintered at 1600°C; (e) 25vol%, alumina loading slurry sintered at 1400°C and (f) 25vol%, alumina loading slurry sintered at 1600°C**

The strut thickness and the pore filling was more in the sample prepared with a slurry having 35vol% alumina loading (Fig 6.32(c)) as compared to that of Fig. 6.32[(a) and (b)] (Sample prepared with a slurry having 25vol% and 30vol% alumina loading respectively). The increase in strut thickness and pore filling is attributed to the increased alumina slurry coating thickness of the template. SEM micrographs of the samples prepared with 25vol% alumina loading slurry sintered at 1400, and 1600°C has also been shown in Fig. 6.31 (e) and (f) respectively. It could be observed from micrographs that the grain size of the alumina was small in Fig 6.31(e) as compared to that observed in Fig 6.32(f). The population of intergranular porosity was found to be more in Fig 6.32(e) as compared to that observed in micrograph Fig 6.32(f). The increase in the pore population is correlated to the densification of the samples. The samples sintered at low temperature (1400°C) are expected to have more porosity and the samples sintered at high temperature are expected to have exaggerated grain size. Thus, the samples sintered at low temperature (1400°C) showed more porosity. From Fig 6.32(f) the observed exaggerated grain growth is due to the enhanced densification of the samples at elevated temperature (1600°C).

## 6.5. Combination of SRT and SCC Methods

Fabrication of the porous samples with hierarchical pore structure can be possible by the combining the starch consolidation technique (SCC) and the sponge replica technique (SRT). A porosity of 20-70% can be obtained by the SCC technique while the SRT technique can obtain a porosity of 70-90%. Pore size varies in the range of 2-170µm in SCC while pore size varies from 200µm-3mm in SRT. In the SCC method, corn starch granules were used as the gelling – cum – binder – cum pore former. The reaction of the corn starch with water provided the necessary gelling and binding action. The removal of corn starch during sintering resulted in the formation of the porous body. The high strength appears to be due to the presence of starch which partially dissolved in the slurry helping in better packing and densification of the green body. The microstructures (Fig. 6.24) show that the pores are open, but they are isolated and with very few interconnections. As a result, the strength of the porous body was high (27.5 MPa) even at the highest starch content (50 vol% w.r.t alumina loading). On the other hand, in SRT method, the pores were open and interconnected, and the strength was low (2.46 MPa) in comparison to SCC method.

The basic idea of using the combination technique (SRT + SCC) was to develop a hierarchical porous structure. In SRT technique, the maximum porosity obtained was 75%. Thus, only 25% was the solid volume. 3Wt% PVA was added to the slurry to increase the green strength. Thus, the porosity generated due to PVA was ~11%. However, the small sized pores formed from the PVA burn out mostly disappear during sintering. Hence, the majority of the porosity obtained in SRT technique was due to the PU template only. In the combination method (SRT + SCC), the slurry had a total solid loading of 25%. Since, 30 vol% starch (wrt alumina loading) was added to the slurry, this implied that the actual alumina loading is only 17.5 vol%. Thus, the additional porosity generated from starch was 7.5% only. A part of the starch will react with water and do the binding action. Therefore, it can be assumed in the combination technique, 5% additional porosity could be realized through starch addition. However, it was also observed that this increase in the porosity did not adversely affect the strength in a significant way. Thus, the combination of SRT + SCC method resulted in the development of a hierarchical porous structure containing macro and meso pores without a significant decrease in the strength.

### 6.5.1. Volume Shrinkage

Sintered volume shrinkage at 1400°C of the porous alumina samples prepared by combination technique has been shown in the Fig 6.33 as a function of alumina loading of the slurry containing 30vol% corn starch.

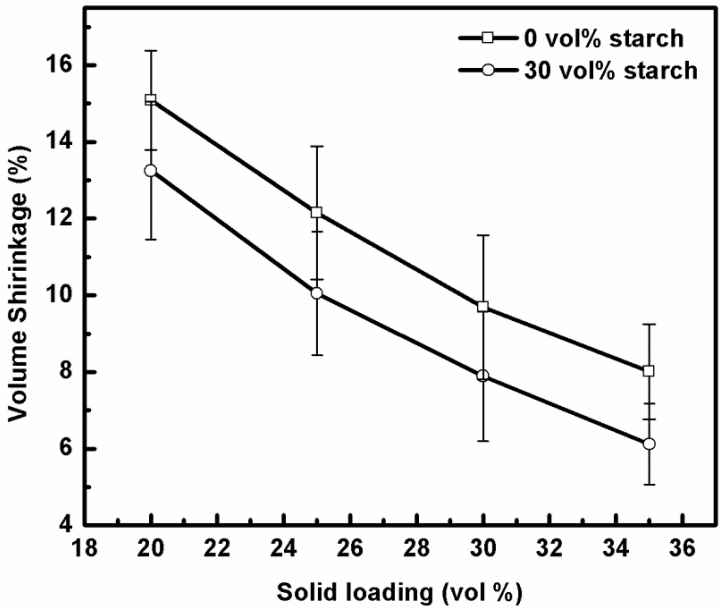


**Figure 6.33 Volume shrinkage of the sample prepared by combination technique as a function of alumina loading in the slurry containing 30 vol% starch.**

Sintered volume shrinkage values of the samples prepared by sponge replica technique have also been plotted in the figure for comparison. It has been observed that the volume shrinkage decreases with the increase in the alumina loading. With the increase in alumina loading from 20-35 vol %, the shrinkage decreased from 13-6% in the presence of starch and 15-8% without starch respectively.

The decrease in the shrinkage with solid loading has been attributed to the increase in the packing of the alumina particles as explained earlier. The shrinkage increased from 13-15% with the addition of starch. Small size pore former pores are likely to be formed in the samples prepared with corn starch due to distributed particle size of the starch. These small size pores disappear easily during sintering as compared to that having a large size. Hence, the more shrinkage is observed in the samples with the starch content compared to the samples without starch.

### 6.5.2. Apparent Porosity

The influence of the alumina loading of a slurry containing 30vol% corn starch on the apparent porosity of porous alumina ceramics samples fabricated by combination technique is presented in the Fig 6.34.

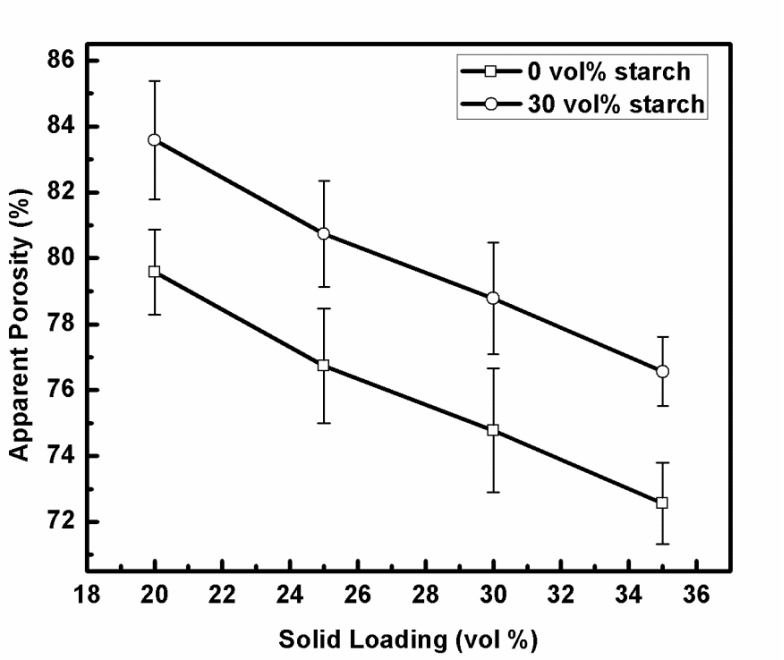


**Figure 6.34 Apparent porosity of the sample prepared by combination technique as a function of alumina loading in the slurry containing 30 vol% starch.**

The samples were sintered at 1400°C. Apparent porosity of the samples prepared with sponge replica technique has also been inserted in the figure for ready reference. It has been observed that the porosity decreases with the increase in the $Al_2O_3$ loading. The decrease in porosity with an increase in alumina loading is correlated with an increase in packing density and/or increase in strut/pore wall thickness with an increase in alumina loading in the slurry. It could also be observed that the porosity increases with increase in starch content in the slurry. The apparent porosity increases from 79-83.5% at 20vol% alumina loading and from 72-76% at 35vol% solid loading with the addition of 30vol% starch. The increase in porosity with starch content is due to the formation of pore former porosity from the burn out of the starch.

### 6.5.3. Cold Crushing Strength

Cold crushing strength (CCS) of the sample fabricated using combination technique as a function of alumina loading of the slurry containing 30vol% starch is shown in Fig 6.35.

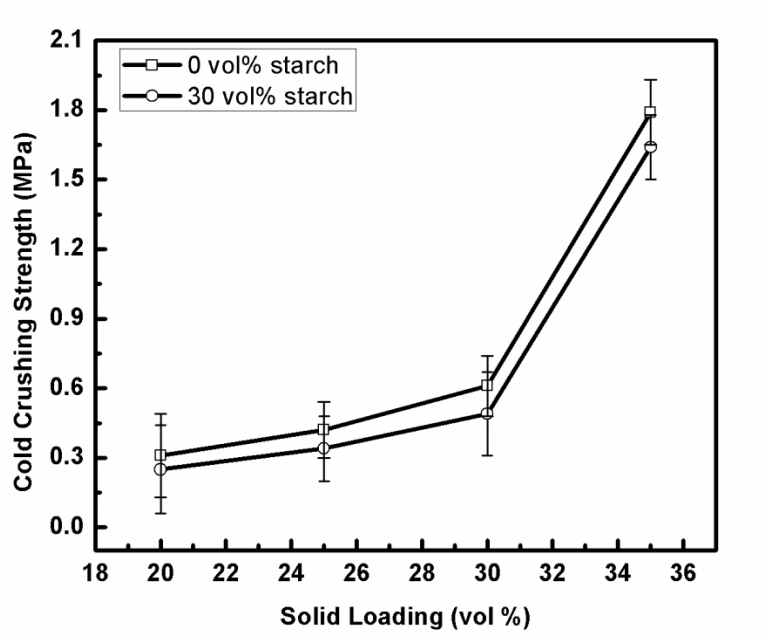


**Figure 6.35 Cold crushing strength of the sample prepared by combination technique as a function of alumina loading in the slurry containing 30 vol% starch.**

Strength values of the samples prepared without starch addition has also be included in the figure for comparison. All the samples were sintered at 1400°C. It has been observed that the CCS of the samples increases with increase in alumina loading of the slurry. A similar behavior as that observed in the samples prepared by sponge replica technique and could be correlated with the strut and pore wall thickness increase as well as the density of the sample (as explained earlier). It is worthy to note that the strength of the sample was decreased with the incorporation of starch in the slurry. The starch addition in the slurry as likely to generate pore on the strut as well as pore wall. The microstructural study revealed the existence of small interconnected pores at struts and pore walls. Thus, the strength decreases with the addition of starch to the slurry.

### 6.5.4. Microstructure

The microstructure of the porous alumina samples fabricated by the combination of the starch consolidation and polymeric sponge replica technique has been shown in the Fig 6.36. The microstructure of the samples prepared from 25vol%, 30vol% and 35vol% alumina loaded slurry containing 30 vol% corn starch are shown in the Fig 6.36 [(a) - (c) respectively]. Samples were sintered at 1400°C. Large interconnected pores, the characteristics of sponge replica could easily be observed from all the micrographs. It could also be observed that with an increase in alumina loading the strut and the pore wall thickness of the samples increases.

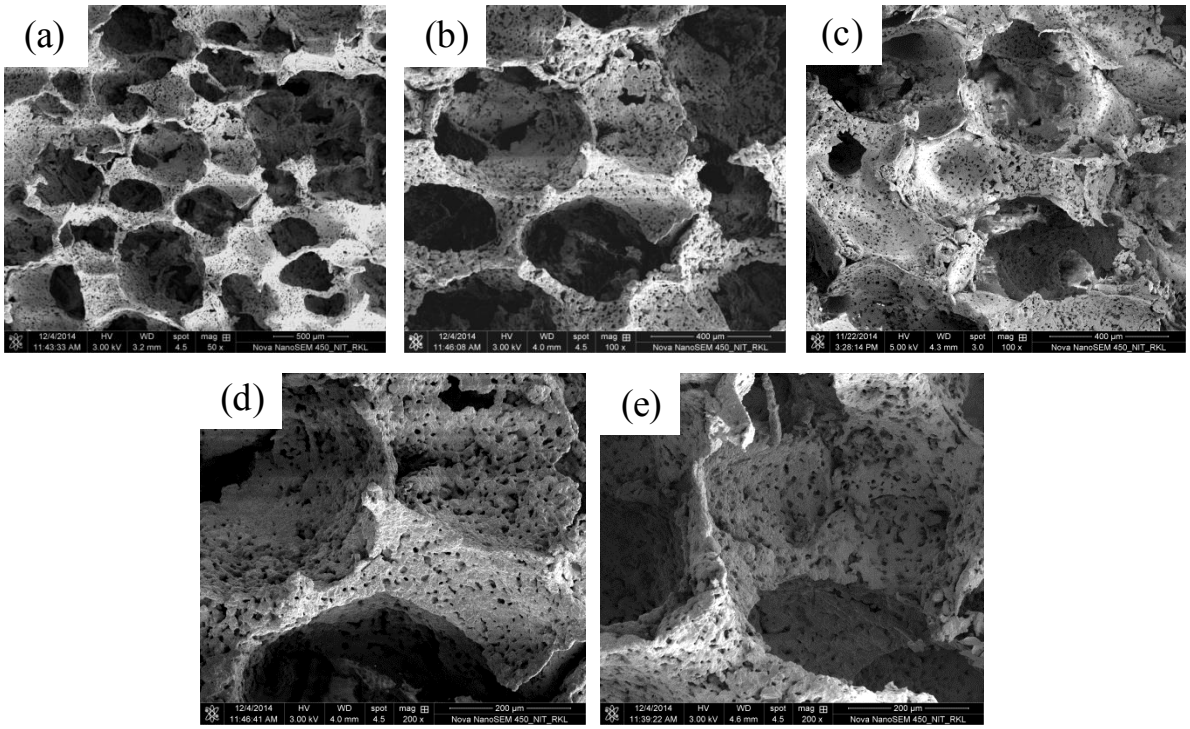


**Figure 6.36 SEM Micrographs of the samples sintered at 1600°C prepared by combination technique as a function of alumina loading [(a) 25 vol% ,(b) 30 vol% ,(c) 35 vol% ] and starch content[(d) 20 vol% ,(e) 30 vol% ].**

The increase in strut thickness and pore wall thickness with an increase in alumina loading could be explained in the same line as discussed earlier. A magnified micrographs indicating the presence of small interconnected pores on the strut and pore wall has also been presented in Fig 6.36[(d) and (e)]. The samples have been prepared with 30vol% and 40vol% corn starch added in 20vol% alumina slurry. The presence of the small interconnected pores at strut and pore wall confirms the formation of hierarchical porosity in the samples fabricated by a combination of SCC and SRT techniques. It could also be observed that with the population of the small interconnected pores increases with increase in the starch content of the slurry and could be correlated with the typical characteristics of the starch consolidation technique. These small interconnected pores are correlated to the pore former porosity created from the burn out of the starch used. The formation of interconnected pores at strut and pore walls are attributed to the low strength value observed in these samples (as discussed in the previous section).

# Chapter 7 Conclusions and Scope of Future Work

## 7.1. Conclusion

The present research work discussed the fabrication of the porous alumina ceramics through starch consolidation casting (SCC), sponge replica technique (SRT) and the combination of SCC and SRT techniques. Alumina loading, starch content, starch type of the slurry has been monitored as slurry parameters and sintering temperature as process parameter has been varied to develop porosity in the samples prepared by SCC technique. It was also observed that irrespective of solid loading of the slurry 0.3 wt% Darvan C was sufficient to obtain a stable and dispersed slurry. All the slurry exhibited shear thinning behaviour within the solid loading range 30-45 vol% and starch content in the range 1-50 vol%. The viscosity of the slurry in the range 0.05-1.19 Pa.s was found to be necessary for fabrication of defect-free samples by this technique. Samples casted below this range of viscosity had lamination and high drying shrinkage, while those casted with a viscosity above this range had a blow and pin holes. The properties of the green starch consolidated ceramics could be explained condidering i) water content or more precisely free water content and ii) volume stress developed during consolidation due to swelling of the starch. The physical properties of sintered starch consolidated ceramics depend on alumina loading as well as starch content in the slurry. Strength and porosity of the samples follows an inverse relationship. Sintering at high temperature resulted in more densification of the samples leading to a decrease in porosity and increase in strength. Starch content in the slurry is more effective in controlling the porosity of the samples as compared to that of alumina loading of the slurry. The porosity of the samples could be varied from 20-70% in this technique. When 3 wt% $TiO_2$ was added to alumina, it acted as a sintering aid with a consequent reduction in the sintering temperature by 300$^{o}$C. The enhanced densification was achieved without compromising the strength and porosity of the samples fabricated by this technique and could be able to develop ceramics with as low as 10% porosity. The porosity of starch consolidated ceramics could be well predicted by the theoretical model presented in the present study.

It was found that a slurry viscosity between 0.055-0.378 Pa.s was effective in achieving an uniform coating of slurry on the sponge template. The uniformity of coating could be varied either by varying alumina loading or by varying the PVA content in the slurry. The strength of SRT samples increased with increase in temperature as well as with alumina solid loading along with a concurrent decrease in porosity.

The porosity of the samples could be varied from 75- 80% of strength 0.31-2.46 MPa by this technique when fabricated with 20 vol% $Al_2O_3$ solid loading, one wt% $TiO_2$ containing slurry sintered at 1400°C.

Hierarchical porosity could be obtained in the samples prepared by the combination technique (SCC+SRT) as revealed from its microstructure. Thus, samples with porosity in the range 10-80% could be fabricated by the above techniques.

### 7.2. Scope of future work

1. The pore size, shape, and its distribution in the samples needs to be carried in order to comment on the possible applications of these ceramics.
2. Water or gas permeability measurements for these macroporous ceramics need to be studied in order to ascertain their interconnectivity.
3. Sponge morphology is an important parameter to tailor the microstructure of the sample prepared by SRT technique. Thus, further study on the sample prepared with a different sponge (differing morphological aspect) is required in this regard.
4. Hierarchical porosity although could be produced by combination technique, further study dealing with the effect of starch type, starch content, starch particle size, etc. on the pore morphology is required.

# Chapter 8 References

1. A.R. Studart., T. Gonzenbach., E. Tervoort., L.J. Gauckler, "**Processing routes to macroporous ceramics: a review**", J. Am. Ceram. Soc., 89(2006) 1771–1789.
2. Z. Taslicukur, C. Balaban, N. Kuskonmaz, "**Production of foam filters for molten metal filtration using expanded polystyrene**," J. Eur. Ceram. Soc. 27 (2007) 637-640.
3. Nandini Das and H. S. Maiti "**Effect of Size Distribution of the Starting Powder on the Pore Size and its Distribution of Tape Cast Alumina Microporous Membranes**" J. Eur. Ceram. Soc. 19 (1999) 341-345.
4. Anne Julbe, David Farrusseng, ChirstianGuizard, "**Porous ceramic membranes for catalytic reactors overview and new ideas**." J. Memb. Sci. 181 (2001) 3-20.
5. O. Lyckfeldt, J. Ferreira, "**Processing of porous ceramics by starch consolidation**", J. Eur. Ceram. Soc. 18 (1998) 131–140.
6. Kalyani Mohanta, Ajay Kumar, Om Parkash, Devendra Kumar "**Processing and properties of low cost macroporous alumina ceramics with tailored porosity and pore size fabricated using rice husk and sucrose**" J. Eur. Ceram. Soc., 34 (2014) 2401-2412.
7. B.P. Saha, Sweety Kumari, R. Johnson and N. Eswara Prasad, "**Effect of relative density on the compressive flow behaviour of cordierite and cordierite- mullite honeycombs**" Transactions of The Indian Institute of Metals vol 63 (2010) pp.701-706.
8. Gang Liu, "**Fabrication of porous ceramics and composites by novel freeze casting process**," PhD Thesis, University of Birmingham, March 2011, p. 25-41.
9. Santanu Dhara and Parag Bhargava "**Egg White as an Environmentally Friendly Low-Cost Binder for Gelcasting of Ceramics**" J. Am. Ceram. Soc., 84 [12] (2001) 3048–50.
10. Xiaolin Liu, Yong Huang, Jinlong Yang, "**Effect of rheological properties of the suspension on the mechanical strength of $Al_2O_3$-$ZrO_2$ composites prepared by gel casting.**" Ceram. Int. 28 (2002) 159-164.
11. B. P. Singh, Sarama Bhattacharjee, Laxmidhar Besra, Dilip K. Sengupta "**Evaluation of dispersibility of aqueous alumina suspension in presence of Darvan C**" Ceramics International 30 (2004) 939–946.
12. P. R. Aravind, P. Mukundan, P. Krishna Pillai, K.G.K. Warrier "**Mesoporous silica–alumina aerogels with high thermal pore stability through hybrid sol–gel route followed by subcritical drying**" Microporous and Mesoporous Materials 96 (2006) 14–20.
13. E.Gregorova, Willi Pabst, "**Process control and optimized preparation of porous alumina ceramics by starch consolidation casting**." J. Eur. Ceram. Soc., 31 (2011) 2073-2081.
14. Hanyu Yangcheng, "**Characterisation of normal and waxy corn starch for bioethanol production**" Graduate thesis and dissertations, Iowa State University, 2012, pp.13-19.
15. Iis Sopyan, Jasminder Kaur, "**Preparation and characterization of porous hydroxyapatite through polymeric sponge method.**" Ceram. Int. 35 (2009) 3161-3168.
16. M.N.Rahaman, "**Ceramic processing and sintering**" pp. Marcel Dekker Inc, New York, 1998.
17. Fateme Rezaei, Alessandra Mosca, Paul Webley, Jonas Hedlund and Penny Xiao, "**Comparision of traditional and structural absorbents for $CO_2$ separation by vacuum swing adsorption**" Ind. Eng. Chem. Res. 49 (2010) 4832-4841.
18. Avelino Corma, "**From microporous to mesoporous molecular sieve materials and their use in catalysis**" Chem. Rev. 97 (1997) 2373-2419.

19. Gustav Nordlund, Jovice Boon Sing Ng, Lennart Bergstrom and Peter Brzezinski, " **A membrane reconstituted multisubunit functional proton pump on mesoporous silica particles**" Am. Chem. Soc., vol.3 (2009) 2639-2646.
20. Jenny Andersson, Jessica Rosenholm, Sami Areve, and Mika Linden, "**Influences of material characteristics on ibuprofen drug loading and release profiles from ordered micro and mesoporous silica matrices**" Chem. Mater. 16 (2004) 4160-4167.
21. M.V.Twigg and J.T.Richardson "**Theory and applications of ceramic foam catalysts**" Trans IChemE, Vol 80 (2002).
22. J.Luyten, S.Mullens, I.Thijs, "**Designing with pores synthesis and applications**" KONA Powder and Partcle journal, 28 (2010).
23. Michele Ambrogio, Guido Saracco, Vito Specchia, "**Combining filtration and catalytic combustion in particulate traps for diesel exhaust treatment**," Chem. Engg. Sci. 56 (2001) 1613-1621.
24. Z. Taslicukur, C. Balaban, N. Kuskonmaz, "**Production of foam filters for molten metal filtration using expanded polystyrene**," J. Eur. Ceram. Soc. 27 (2007) 637-640.
25. J.M.Taboas, R.D.Maddox, P.H.Krebsbach, S.J.Hollister, "**Indirect solid free form fabrication of local and global porous, biomimetic and composite 3D polymer ceramic scaffolds**," Biomaterials 24 (2003) 181-194
26. Anne Julbe, David Farrusseng, Chirstian Guizard, "**Porous ceramic membranes for catalytic reactors – overview and new ideas**," J. Memb. Sci. 181 (2001) 3-20.
27. Asad U.Khan, Brian J.Briscoe, Paul F.Luckham "**Interaction of binders with dispersant stabilized alumina suspensions**" Colloids and surfaces, Physicochemical and Engineering aspects, 161 (2000) 243-257.
28. F.A.Almeida, E.C.Botelho, F.C.L.Melo, T.M.B.Campos, G.P.Thim, "**Influence of cassava starch content and sintering temperature on the alumina consolidation technique**." J. Eur. Ceram. Soc. 29 (2009) 1587-1594.
29. JunIchiro Tsubaki, Masanobu Kato, Masanori Miyazawa, Takuya Kuma, Hidetoshi Mori "**The effects if the concentration of a polymer dispersant on apparent viscosity and sedimentation behavior of dense slurries**." Chem. Engg. Sci. 56 (2001) 3021-3026.
30. Brian J.Briscoe, Asad U.Khan and Paul F.Luckham, "**Optimising the dispersion on an alumina suspension using commercial polyvalent electrolyte dispersants**" PII (1998) 0955-2219.
31. Athena Tsetsekou et.al. "**Optimization of rheological properties of alumina slurries for ceramic processing applications. Part -1: slip casting**." J. Eur. Ceram. Soc., 21 (2001)363-373.
32. H.M. Alves, G.Tari, A.T.Fonseca and J.M.F. Ferreira "**Processing of porous cordierite bodies by starch consolidation**", Mater. Res. Bull. 33 (10) (1998) 1439-1448.
33. A.F.Lemos and J.M.F. Ferreira "**Porous bioactive calcium carbonate implants processed by starch consolidation**", Mater. Sci. Eng. C11 (1) (2000) 35-40.
34. Zuzana Zivcova Eva Gregorova, Willi Pabst, "**Alumina ceramics prepared with new pore forming agents**" processing and applications of ceramics, 2[1] (2008)1-8.
35. Aranzazu Diaz, Stuart Hampshire, "**Characterization of porous silicon nitride materials produced with starch**", J. Eur. Ceram. Soc. 24 (2) (2004) 413-419.

36. Rafael Barea, Maria Isabel Osendi, J.M.F. Ferreira, Pilar Miranzo, "**Thermal conductivity of highly porous mullite material**", Acta. Mater. 53 (11) (2005) 3313-3318.
37. J.G.Kim, J.H.Sim, W.S.Cho, "**Preparation of porous (Ba,Sr)TiO3 by adding corn starch**", J. Phys. Chem. Solids 63 (11) (2002) 2079-2084.
38. W.Pabst, E.Tynova, J.Mikac, E.Gregova, J.Havrda "**A model for the body formation in starch consolidation casting**" J. Mat. Sci. Let. 21 (2002) 1101-1103.
39. J.L.Minatti, J.G.A.Santana, R.S.Fernandes, E.Campos "**Alumina developed by pre gelling starch consolidation (PSC)**." J. Eur. Ceram. Soc., 29(2009) 661-668.
40. Jaroslav Blazek, Les Copeland "**Pasting and swelling properties of wheat flour and starch in relation to amylose content**" Carbohydrate Polymer, 71 (2008) 380-387.
41. Sathaporn Srichuwong Titi Candra Sunarti, Takashi Mishima, Naoto Isono, Makoto Hisamatsu, "**Starches from different biological sources – contribution of starch structure to swelling and pasting properties**." Carbohydrate polymers 62 (2005) 25-34.
42. P.Aggarwal, D.Dollimore and K.Heon "**Comparative thermal analysis study of two biopolymers, starch and cellulose**" J. Thermal Analysis 50 (1997) 7-17.
43. Sa Li, Chang-An Wang, Jun Zhou, "**Effect of starch addition on microstructure and properties of highly porous alumina ceramics**." Ceram.Int. 39 (2013) 8833-8839.
44. K.Prabakaran, Anand Melkeri, N.M. Gokhale, S.C.Sharma "**Preparation of macroporous ceramics using wheat particles as gelling and pore forming agent**" Ceram.Int. 33 (2007) 77-81.
45. Lunlun Gong, Yonghong Wang, Xudong Cheng, Ruifang Zhang, Heping Zhang "**Porous mullite ceramics with low thermal conductivity prepared by foaming and starch consolidation**" J. Porous Mater (2013).
46. Xiaojian Mao, Shiwei Wang, Shunzo Shimai "**Porous ceramics with tri modal pores prepared by foaming and starch consolidation**" Ceram.Int. 34 (2008) 107-112.
47. James S Reed "**Principles of ceramic processing**" pp. 279-282 John Wiley ans Sons, Inc. US, 1995.
48. Eva Gregorova, Willi Pabst, Zuzana Zivcova, Ivona Sedlarova, Svatava Holikova, "**Porous alumina ceramics prepared with wheat flour**" J. Eur. Ceram. Soc., 30 (2010) 2871-2880.
49. M.H.Talou, M.A.Camerucci, R.Moreno, "**Rheology of aqueous mullite-starch suspensions**" J. Eur. Ceram. Soc., 31 (2011) 1563-1571.
50. J.Chandradass, Ki Hyeon Kim, Dong Sik Bae, K.Prasad, G.Balachandar, S.Athisaya Divya, M.Balasubramanian, "**Starch consolidation of alumina: fabrication and mechanical properties**." J. Eur. Ceram. Soc., 29 (2009) 2219-2224.
51. R.M. Khattab, M.M.S. Wahsh,N.M. Khalil " **Preparation and characterization of porous alumina ceramics through starch consolidation casting technique** ." Ceram. Int. 38, (2012) , pp.(4723–4728).
52. Zuzana Zivcova- Vickova, Janis Locs, Melanie Keuper, Ivona Sedlafova, Michaela Chmelickova, "**Microstryctural comparison of porous oxide ceramics from the system Al2O3-ZrO2 prepared with starch as a pore forming agent**" J. Eur. Ceram. Soc., 32 (2012) 2163-2172.
53. W.Pabst, E.Gregorova, I.Sedlafova, M.Cerny, "**Preparation and characterization of porous alumina zirconia composite ceramics**" Ceram.Int. 31 (2011) 2721-2731.

54. M.H.Talou, M.A.Villar, M.A.Camerucci "**Thermogelling behaviour of starches to be used in ceramic consolidation process**" Ceram.Int. 36 (2010) 1017-1026.
55. E.Gregorova, W.Pabst, "**Porous ceramics prepared using poppy seed as a pore forming agent**" Ceram.Int. 33 (2007) 1385-1388.
56. E. Gregorova, W. Pabst, "**Porosity and pore size control in starch consolidation casting achievements and problems**", J. Eur. Ceram. Soc. 27, 2007, (669–672).
57. Hilkart Erkalfa, Zulal Misirli and Tarik Baykara, "**Densification of alumina at 1250°C with $MnO_2$ and $TiO_2$ additives**" Ceram.Int. 21 (1995) 345-348.
58. M.Sathiya Kumar, F.D.Gnanam, "**Influence of MnO and $TiO_2$ additives on density, microstructure and mechanical properties of $Al_2O_3$**" Ceram.Int. 28 (2002) 195-200.
59. June Ho Park, Young Hag Koh, Hyoun Ee Kim and Cheol Seong Hwang "**Densification and mechanical properties of titanium diboride with silicon nitride as a sintering aid**" J.Am.Ceram.Soc., 82 (1999) 3037-42.
60. Long Hao Li, Hyoun Ee Kim, Eul Son Kang "**Sintering and mechanical properties of titanium diboride with aluminum nitride as a sintering aid**" J. Eur. Ceram. Soc., 22 (2002) 973-977.
61. M.Sathiya Kumar, F.D.Gnanam, "**Influence of additives on density, microstructure and mechanical properties of alumina**" J. Mater. Processing Tech, 133 (2003) 282-286.
62. Yong-sheng Han, Jian-bao Li, Qiang-min Wei, Ke Tang, "**The effect of sintering temperatures on alumina foam strength**." Ceram. Int. 28 (2002) 755-759.
63. Xinwen Zhu, "**The control of slurry rheology in the processing of recticulated porous ceramics**" material research bulletin 37 (2002), 541-553.
64. Hassna Rehman Ramay, Miqin Zhang "**Preparation of porous hydroxyapatite scaffolds by combination of the gel casting and polymer sponge methods**" Biomaterials 24 (2003) 3293-3302.
65. Xiumin Yao, Shouhong Tan, Zhengren Huang, Dongliang Jiang "**Effect of recoating slurry viscosity on the properties of reticulated porous silicon carbide ceramics**" Ceram. Int. 32 (2006) 137-142.
66. Xinwen Zhu, Dongliang Jiang, Shouhong Tan, "**Improvement in the strength of reticulated porous ceramics by vacuum degassing**" Materials Letters 51 (2001) 363-367.
67. Sathaporn Srichuwong Titi Candra Sunarti, Takashi Mishima, Naoto Isono, Makoto Hisamatsu, "**Starches from different botanical sources I- contribution of amylopectin fine structure to thermal properties and enzyme digestibility.**" Carbohydrate polymers 60 (2005) 529-538.
68. Ahmad Fadli, Iis Sopyan, "**porous ceramics with controllable properties prepared by protein foaming consolidation method**" J. Porous Mater 18 (2011) 195-203.
69. L.B.Garrido, M.P.Albano, K.P.Pluknett, L.Genova, "**Effect of starch filler content and sintering temperature on the processing of porous 3Y-ZrO2 ceramics**" J. Mater. Proc. Tech. 209 (2009) 590-598.
70. Chih-JenWang, Chi-Yuen Huang, "**Effect of TiO2 addition on the sintering behavior, hardness and fracture toughness of an ultrafine alumina**." J. Mat. Sci. Eng. A 492 (2008) 306-310.
71. R.D. Bagley, I.B. Cutler, D.L. Johnson, J. Am. Ceram. Soc. 53 (3) (1970) 136–141.
72. K. Hamano, C.S.Hwang, Z.Nakagawa,Y.Ohya, Jpn. Ceram. 94 (5) (1986) 505–511.
73. R.J. Brook, J. Am. Ceram. Soc. 55 (2) (1972) 114–115.